

# Optical Indicators and Molecular Probes

## Developed at Regensburg University

vs. of 16-Jan-2021; edited by O. S. Wolfbeis

This group of compounds and nanoparticles includes indicator probes (molecular probes and nanoparticle probes). Unlike labels, they are supposed to respond to (bio)chemical species or to parameters in their environment. They can be used to quantify (a) a chemical parameter (such as oxygen, pH value or the concentration of calcium ion), (b) a biochemical parameter (such as the presence if not concentration of DNA, or the activity of an enzyme), or (c) a physical parameter such as temperature, pressure, or solvent or cell membrane polarity. Such probes are widely applied in clinical studies and cell biology, but also in industry. The list does not contain papers on complete optical sensor devices.

## Sections

1. Probes for Molecular Oxygen
  2. Probes for pH Values
  3. Probes for Temperature
  4. Probes for Hydrogen Peroxide
  5. Probes for Enzyme Activity, Inhibition Assays, and Enzymatic Assays of Substrates
  6. Probes for DNA and (Bio)phosphates (incl. inorganic phosphates)
  7. Probes for Halides (mainly chloride)
  8. Probes for Metal Ions (mainly alkali ions and heavy metal ions)
  9. Probes for Organic Species
  10. Lipid Probes (usually probes for membranes, micelles or surfactants)
  11. Solvent Polarity Probes
  12. Albumin Probes
- 

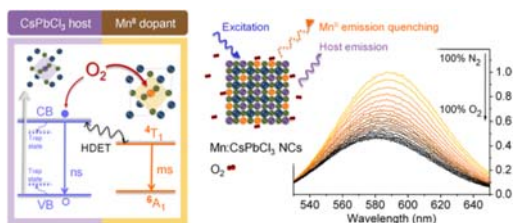
## Section 1. Probes for Molecular Oxygen

**602. Mn(II)-Doped Cesium Lead Chloride Perovskite Nanocrystals: Demonstration of Oxygen Sensing Capability Based on Luminescent Dopants and Host-Dopant Energy Transfer.** F. Lin, F. Li, Z. Lai, Z. Cai, Y. Wang, O. S. Wolfbeis, X. Chen. *ACS Appl. Mat. Interfaces* (2018), 10, 23335-23343. DOI: 10.1021/acsami.8b06329. IF: 8.5.

**Abstract:** We demonstrate the O<sub>2</sub> sensing capability of Mn(II)-doped CsPbCl<sub>3</sub> nanocrystals (Mn:CsPbCl<sub>3</sub> NCs) and reveal the role of O<sub>2</sub> on the optical de-excitation of such perovskite nanocrystals (PNCs). By adjusting the amount and distribution of Mn(II) dopants, as well as the host-dopant energy transfer (HDET) process in PNCs, we highlight that O<sub>2</sub> can reversibly quench the Mn(II) emission due to their temporarily disturbance to the ligand field of near-surface dopants in PNCs. In the phosphorescence mode, the PL of the NCs is quenched by 53% on going from 0 to 100% of O<sub>2</sub>. The Stern-Volmer plot is linear in the 0-12% O<sub>2</sub> concentration range. High sensing reversibility and rapid signal response are also achieved. In our perception, the mechanism study makes these PNCs well suited as optical probes for O<sub>2</sub>, and it is enlightening to explore more possibilities of the inherent O<sub>2</sub> sensing based on semiconductor doped-NCs (not restricted to Mn-doped PNCs) with phosphorescence emission.

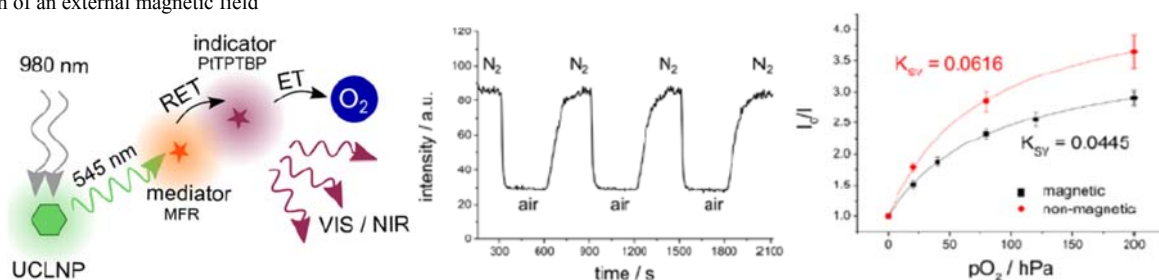


Figures of merit: Abs: 365 nm. Em: (yellow): 585 nm.  $\tau$  between 1 and 2 ms. Net formula:  $\text{Mn}:\text{CsPbCl}_3$ .



**592. Composite Particles with Magnetic Properties, Near-Infrared Excitation, and Far-Red Emission for Luminescence-Based Oxygen Sensing.** E. Scheucher, S. Wilhelm, O. S. Wolfbeis, T. Hirsch, T. Mayr, *Microsyst. Nanoeng.* (2016), vol. 1, 15026. DOI: 10.1038/micronano.2015.26. Open access.

**Abstract:** Oxygen sensing, magnetic and upconversion luminescence properties are combined in multi-functional composite particles prepared herein by a simple mixing, baking and grinding procedure. Upconverting nanocrystals are used as an excitation source and an oxygen indicator with far-red emission. The composite particles are excited with near infrared laser light (980 nm). The visible upconversion emission is converted into an oxygen concentration-dependent far-red emission ( $< 750 \text{ nm}$ ) using an inert mediator dye and a platinated benzoporphyrin dye. This concept combines the advantages of NIR excitation and far red emissive indicator dyes, offering minimized auto-fluorescence and enhanced membrane permeability. Additional functionality is obtained by incorporating magnetic nanoparticles into the composite particles, which enables easy manipulation and separation of the particles by the application of an external magnetic field



**587. Review: Luminescent Sensing and Imaging of Oxygen: Fierce Competition to the Clark Electrode.** O. S. Wolfbeis, *Bioessays* (2015) 37(8), 921-928. DOI: 10.1002/bies.201500002. IF: 4.7. Open access.

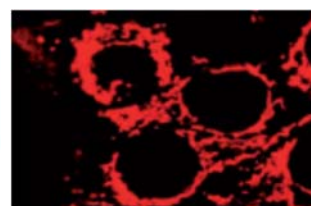
**Abstract:** Luminescence-based sensing schemes for oxygen have experienced a fast growth and are in the process of replacing the Clark electrode in many fields. Unlike electrodes, sensing is not limited to point measurements via fiber optic microsensors, but includes additional features such as planar sensing, imaging and intracellular assays using nanosized sensor particles. This essay discusses, in layman's terms, (a) the common solid-state sensor approaches based on the use of indicator dyes and host polymers; (b) fiber optic and planar sensing schemes as well as nanoparticle-based intracellular sensing; and (c) common spectroscopies. Optical sensors also are capable of multiple simultaneous sensing (such as  $\text{O}_2$  and temperature). Sensors for  $\text{O}_2$  are produced nowadays in large quantities. Fields of application include plant and animal physiology, clinical chemistry, marine sciences, the chemical industry and process biotechnology.



Optoelectronic system containing an RSB port (left) and a fiber connector (right) for fiber optic decay time-based sensing of  $\text{O}_2$ .



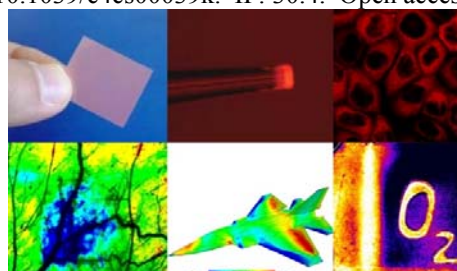
Schematic of the state of the art in imaging  $\text{O}_2$ . Left: PC with software and for display. Center: Handheld portable instrument for lifetime imaging. Red film: Sensor membrane incorporated with a quenchable luminescent probe for  $\text{O}_2$  to be placed on the object of interest (a bioreactor, or skin, or an aircraft, etc.; symbolized by a cube)



Imaging of mitochondrial  $\text{O}_2$  in cells using sensor NPs. Pictures are comparable to those obtained with a mitotracker but luminescence intensity depends on local  $p\text{O}_2$

**578. Review: Optical Methods for Sensing and Imaging Oxygen: Materials, Spectroscopies and Applications.** X. Wang, O. S. Wolfbeis; *Chem. Soc. Rev.* (2014), 43, 3666-3761. DOI: 10.1039/c4cs00039k. IF: 30.4. Open access.

**Abstract:** We review the current state of optical methods for sensing oxygen. These have become a powerful alternative to electrochemical detection and are in the process of replacing the Clark electrode in many fields. The article (with 693 refs.) is divided into main sections on direct spectroscopic sensing of oxygen, on absorptiometric and luminescent probes, on polymeric matrices and supports, on additives and related materials, on spectroscopic schemes for read-out and imaging, and on sensing formats (such as waveguide sensing, sensor arrays, multiple sensors and nanosensors). We finally discuss future trends and applications and summarize the properties of the most often used indicator probes and polymers. A Supporting Information (with 385 refs.) gives a selection of applications of such sensors in medicine, biology, marine and geosciences, in intracellular sensing, aerodynamics, industry and biotechnology, among others.

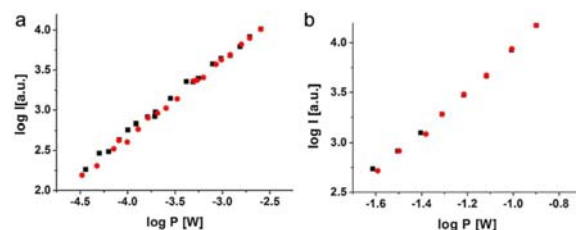




**569. Imaging of Cellular Oxygen via Two-Photon Excitation of Fluorescent Sensor Nanoparticles.** X. Wang, D. E. Achatz, C. Hupf, Sperber, J. Wegener, S. Bange, J. M. Lupton, O. S. Wolfbeis; *Sensors & Actuat., B (Chem.)* (2013), 188, 257-262. DOI: 10.1016/j.snb.2013.06.087. IF: 3.8.

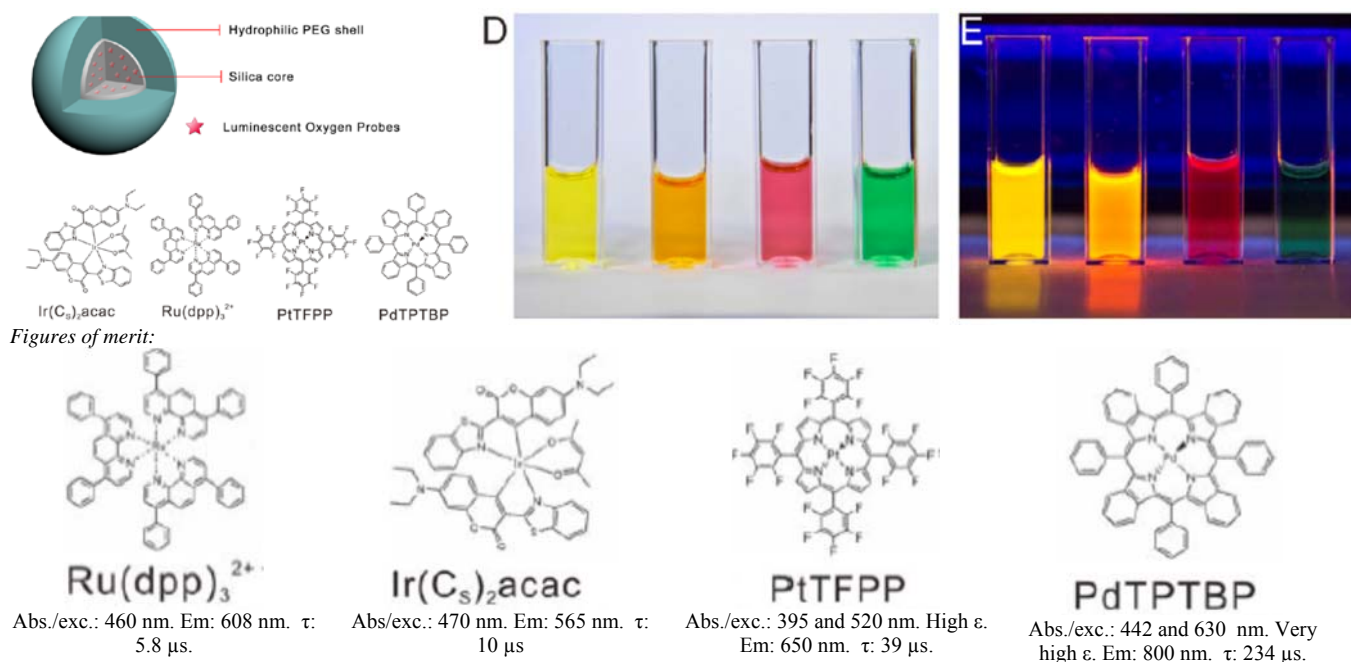
**Abstract:** Polystyrene nanoparticles (PSNPs) with an average size of 85 nm and loaded with an oxygen-quenchable luminescent ruthenium complex were used to image oxygen inside cells following 2-photon excitation (2-PE). The ruthenium probe possesses a large 2-photon absorption cross-section, and 2-PE is achieved by irradiation in the near infrared with fs-pulsed laser systems.

The luminescence of the dye-loaded PSNPs is strongly quenched by oxygen, and Stern–Volmer plots are linear for both conventional 1-PE and for 2-PE. The particles are readily taken up by mammalian cells (MCF-7), presumably via membrane mediated pathways. The 2-PE is considered to be advantageous over conventional imaging techniques because it works in the near-infrared where background absorption and luminescence of biomatter is much weaker than at excitation wavelengths of <600 nm. The Fig. shows double-logarithmic plots of laser power versus emission intensity of the oxygen probe Ru(dpp). Plot (a): excitation via single-photon absorption; the slope is 0.95. Plot (b): excitation via 2-PE (slope 2.04).



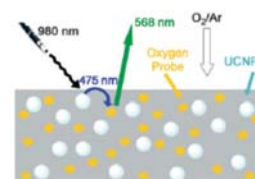
**566. Ultra-Small, Highly Stable, and Membrane-Impermeable Fluorescent Nanosensors for Oxygen.** X. Wang, J. A. Stolwijk, M. Sperber, R. J. Meier, J. Wegener, O. S. Wolfbeis; *Meth. Appl. Fluoresc. (IOP Publ.; London)* (2013), 1, 035002 (7 pp). DOI: 10.1088/2050-6120/1/3/035002.

**Abstract:** We report on the preparation of ultra-small fluorescent nanosensors for oxygen via a one-pot approach. The nanoparticles have a hydrophobic core capable of firmly hosting hydrophobic luminescent oxygen probes. Their surface is composed of a dense and long-chain poly(ethylene glycol) shell, which renders them cell-membrane impermeable but yet highly sensitive to oxygen, and also highly stable in aqueous solutions and cell culture media. These features make them potentially suitable for sensing oxygen in extracellular fluids such as blood, interstitial and brain fluid, in (micro) bioreactors and micro- or nanoscale fluidic devices. Four kinds of nanosensors are presented, whose excitation spectra cover a wide spectral range (395 – 630 nm), thus matching many common laser lines, and with emission maxima ranging from 565 to 800 nm, thereby minimizing interference from background luminescence of biomatter. The unquenched lifetimes are on the order of 5.8 – 234  $\mu$ s, which – in turn – enables lifetime imaging and background separation via time-gated methods. The long decay time of 234  $\mu$ s makes the Pd(II) complex a very sensitive oxygen nanoprobe. The Figure below shows (on the left) the architecture of the ultra-small oxygen-sensitive nanoparticles (NPs) and the chemical structures of the oxygen indicators. (D) shows photographic pictures of oxygen nanosensors in aqueous solutions under ambient light; (E) shows the same cuvettes under UV light. From left to right: Ir-NPs, Ru-NPs, Pt-NPs and Pd-NPs, respectively.



**518. Luminescent Sensing of Oxygen Using a Quenchable Probe Along with Upconverting Nanoparticles.** D. E. Achatz, R. J. Meier, L. H. Fischer, O. S. Wolfbeis; *Angew. Chem. Intl. Ed.* (2011), 50, 260-263. DOI: 10.1002/anie.201004902. IF 12.7.

**Abstract:** We are presenting the first sensor for oxygen that can be excited with NIR light. It makes use of upconverting nanoparticles of the type NaYF<sub>4</sub>: Yb, Tm that are photo-excited with a 980-nm laser and whose visible luminescence is used to photoexcite a quenchable iridium probe for oxygen, thereby overcoming the lack of NIR-excitable probes for oxygen. The components and materials used are readily available, and merits of working at such long excitation wavelength include the complete absence of luminescence background that can be strong in many samples to be analyzed. A new type of ratiometric readout also is demonstrated.



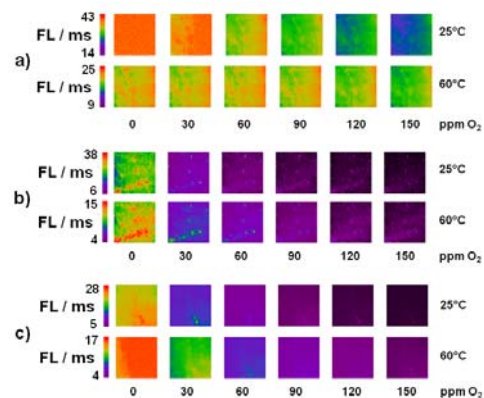
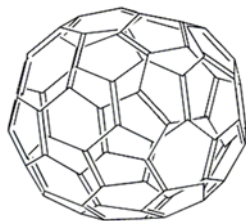
**564. Sensing and Imaging of Oxygen with Parts per Billion Limits of Detection and Based on the Quenching of the Delayed Fluorescence of <sup>13</sup>C<sub>70</sub> Fullerene in Polymer Hosts.** S. Kochmann, C. Baleizão, M. N. Berberan-Santos, O. S. Wolfbeis; *Anal. Chem.* (2013), 85, 1300-1304. DOI: 10.1021/ac303486f. IF: 5.9.



**Abstract:** The method for sensing trace oxygen in the gas phase is based on the extreme efficiency of the quenching of the thermally activated delayed fluorescence of isotopically enriched (85%) carbon-13 fullerene  $C_{70}$  ( $^{13}C_{70}$ ). The fullerene was dissolved in polymer matrices of varying oxygen permeability, viz. polystyrene (PS), ethyl cellulose (EC), and an organically modified silica gel ("ormosil"). The sensor films (5 – 10  $\mu\text{m}$  thick), on photoexcitation at 470 nm, display a strong delayed photoluminescence with peaks between 670 and 700 nm.

Quenching by oxygen was studied at 25 °C and 60 °C, and at levels from zero to 150 ppmv of oxygen in nitrogen gas.

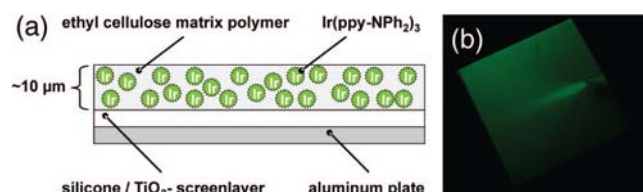
The rapid lifetime determination (RLD) method was applied to determine oxygen-dependent decay times and to perform fluorescence lifetime imaging of oxygen. The oxygen sensors reported here are the most sensitive ones described so far. The color figure shows images based on decay time measurements of  $C_{70}$  in PS, EC and ormosil at various temperatures at



**Figures of merit:**  $\lambda$ : 470 nm;  $\lambda_{\text{em}}$ : 670 – 700 nm.  $\tau$ : 30 – 40 ms. Extremely sensitive probe for oxygen. Based on quenching of the thermally activated delayed fluorescence of isotopically enriched (85%) carbon-13 fullerene  $C_{70}$ . Can detect  $O_2$  gas in concentrations as low as 1 ppm.

#### 483. Exceptional Oxygen Sensing Capabilities and Triplet State Properties of $\text{Ir}(\text{ppy-NPh}_2)_3$ . C. Mak, D. Pentlehner, M. I. J. Stich, O. S. Wolfbeis, W.-K. Chan, H. Yersin; *Chem. Mat.* (2009), 21, 2173-2175. DOI: 10.1021/cm9003678. IF: 5.1.

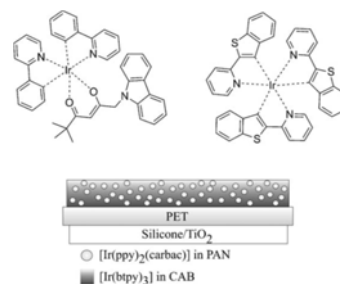
**Abstract:** The oxygen sensing capabilities of a new highly fluorescent iridium complex display favorable sensing properties for oxygen which is due to a relatively long emission lifetime, a high luminescence quantum yield, and a good solubility in organic solvents and in organic polymers. Dissolved in ethyl cellulose, the complex displays high sensitivity to changes of oxygen partial pressure even at air pressures as high as 1500 mbar. The sensor material may be used in fiber optic sensors, in micro-plates, and – if cast onto the surfaces of aircraft models as a thin film; see Fig. (a) – for imaging of air pressure distributions on surfaces. Fig. (b) shows how quenching is suppressed (luminescence lights up) if nitrogen gas is blown over the sensor layer.



#### 485. Red and Green Emitting Iridium(III) Complexes for a Dual Barometric and Temperature Sensitive Paint. L. H. Fischer, M. I. J. Stich, O. S. Wolfbeis, N. Tian, E. Holder, M. Schaeferling; *Chemistry – Eur. J.* (2009), 15, 10857-10863. DOI: 10.1002/chem.200901511. IF: 5.5.

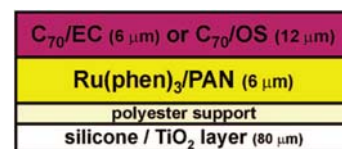
**Abstract:** A dually luminescent paint for measurement of barometric pressure (BP) and temperature ( $T$ ) is presented. The green-emitting iridium(III) complex  $\text{Ir}(\text{ppy})(\text{carbac})$  was applied as a novel probe for  $T$  along with the red-emitting complex  $[\text{Ir}(\text{btpy})]$  which functions as a probe for BP (in fact for oxygen). The two iridium complexes were dissolved in two different polymer materials to achieve optimal responses. The effects of  $T$  on the response of the oxygen probe can be corrected for by simultaneous optical determination of  $T$ . The signals of the probes for  $T$  and BP can be separated by optical filters due to the ~75 nm difference in their emission maxima. The dual sensor is applicable to luminescence lifetime imaging of  $T$  and barometric pressure.

**Figures of merit:** Abs. or exc.: 408 nm ( $\log \epsilon$  4.34; in chloroform). Em: 596, 645 nm.  $\tau$ : 10  $\mu\text{s}$ .



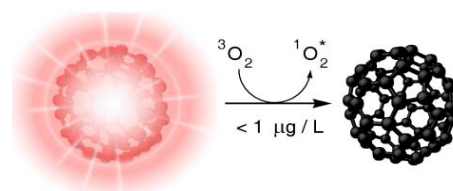
#### 463. Dual Fluorescence Sensor for Trace Oxygen and Temperature with Unmatched Range and Sensitivity, C. Baleizão, S. Nagl, M. Schaeferling, M. N. Berberan-Santos, O. S. Wolfbeis; *Anal. Chem.* (2008), 80, 6449-6457. DOI: 10.1021/ac801034p. IF: 5.6.

**Abstract:** An optical dual sensor for oxygen and temperature ( $T$ ) is presented which is highly oxygen sensitive and covers a broad  $T$  range. It contains two luminescent compounds incorporated into polymer films. Ruthenium tris(1,10-phenanthroline) has a highly  $T$ -dependent luminescence and is incorporated in poly(acrylonitrile) to avoid cross-sensitivity to oxygen. Fullerene  $C_{70}$  was used as the oxygen-sensitive probe owing to its intense thermally activated delayed fluorescence (TADF) at elevated  $T$ 's that is extremely oxygen sensitive. The cross-sensitivity of  $C_{70}$  to  $T$  is accounted for by means of the  $T$  sensor.  $C_{70}$  is incorporated into a highly oxygen permeable polymer, either ethyl cellulose (EC) or organosilica (OS). The two luminescent probes have different emission spectra and decay times and their emissions can be discriminated using both parameters. Spatially resolved sensing is achieved by means of fluorescence lifetime imaging. The dual sensor covers the temp. range from 0 and 120 °C, and detection limits for oxygen are in the low ppbv range. These ranges outperform all dual oxygen and  $T$  sensors reported so far.



#### 447. Optical Sensing and Imaging of Trace Oxygen with Record Response. S. Nagl, C. Baleizão, S. M. Borisov, M. Schaeferling, M. N. Berberan-Santos, O. S. Wolfbeis; *Angew. Chem. Intl. Ed.* (2007), 46, 2317-2319. DOI: 10.1002/anie.200603754. IF: 10.3.

**Abstract:** Ultratrace quantities of oxygen can be determined over a temperature range of more than 100 °C by exploiting the extremely efficient quenching of the delayed fluorescence of fullerene  $C_{70}$  incorporated into organosilica or ethyl cellulose.





Wolfbeis; *Anal. Chem.* **67**, 3160-3166 (1995). DOI: 10.1021/ac00114a010

sample

black optical isolation, 2  $\mu\text{m}$  (optional)

sensor layer, 3 - 5  $\mu\text{m}$  (PS/Ru(dpp))

inert support, ~ 100  $\mu\text{m}$  (PET)

$h\nu_{\text{inc}}$  (blue)       $h\nu_{\text{exc}}$  (red)

ion pair	Ru (diimine)	anion (X)
<b>1a</b>	Ru (dpp) <sub>3</sub>	<i>n</i> -C <sub>12</sub> H <sub>25</sub> SO <sub>3</sub> <sup>-</sup> (DS)
<b>1b</b>	Ru (dpp) <sub>3</sub>	(CH <sub>3</sub> ) <sub>3</sub> SiCH <sub>2</sub> CH <sub>2</sub> CH <sub>2</sub> SO <sub>3</sub> <sup>-</sup> (TSPS)
<b>2a</b>	Ru (phen) <sub>3</sub>	<i>n</i> -C <sub>12</sub> H <sub>25</sub> SO <sub>3</sub> <sup>-</sup> (DS)
<b>2b</b>	Ru (phen) <sub>3</sub>	(CH <sub>3</sub> ) <sub>3</sub> SiCH <sub>2</sub> CH <sub>2</sub> CH <sub>2</sub> SO <sub>3</sub> <sup>-</sup> (TSPS)

<sup>a</sup> dpp, 4,7-diphenyl-1,10-phenanthroline. <sup>b</sup> phen, 1,10-phenanthroline.

**Probes**, I. Klimant, P. Belser, O. S. Wolfbeis; *Talanta* **41**, 985-991 (1994). DOI: 10.1016/0039-9140(94)E0051-R

<i>Oxygen Probe</i>	<i>abs. max.</i>	<i>em. max.</i>	<i>decay time</i>
Ru(bpy)(DMCH) <sub>2</sub> (PF <sub>6</sub> ) <sub>2</sub>	559	742	540
Ru(bpy)(OMCH) <sub>2</sub> (PF <sub>6</sub> ) <sub>2</sub>	532	755	390
Ru(dpp) <sub>2</sub> (DMCH)(PF <sub>6</sub> ) <sub>2</sub>	532	732	640
Ru(dpp)(DMCH) <sub>2</sub> (PF <sub>6</sub> ) <sub>2</sub>	563	738	650

F. Baldini, M. Bacci, I. Klimant, O. S. Wolfbeis; *Sensors Actuat.* **B11** (1993) 347-352. DOI: 10.1016/0925-4005(93)85274-E

Sharma, O. S. Wolfbeis; *Anal. Chim. Acta* **212**, 261-265 (1988). DOI: 10.1016/S0003-2670(00)84148-3

Figure 1 consists of two side-by-side graphs, (a) and (b). Both graphs plot the ratio  $I_T/I$  on the y-axis against oxygen concentration in percent on the x-axis. Graph (a) shows a steep, non-linear increase in the ratio as oxygen concentration increases from 0 to 60%. Graph (b) shows a much flatter, nearly linear increase in the ratio over the same range of oxygen concentration.

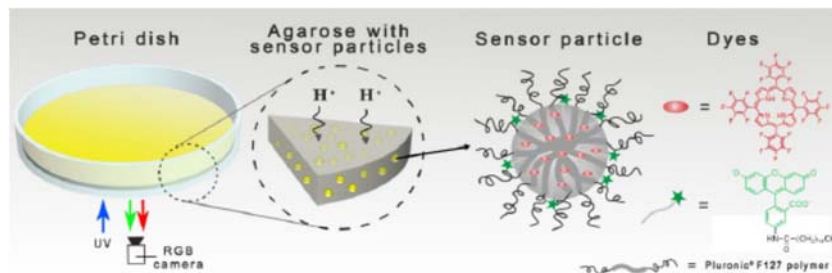
**Partial Pressures**, O. S. Wolfbeis and F. M. Carlini, *Anal. Chim. Acta* **160**, 301-304 (1984). DOI: 10.1016/S0003-2670(00)84535-3



## Section 2. Probes for pH Values

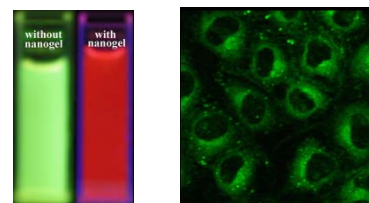
**561. Fluorescent pH-Sensitive Nanoparticles in an Agarose Matrix for Imaging of Bacterial Growth and Metabolism.** X. Wang, R. J. Meier, O. S. Wolfbeis; *Angew. Chem. Int. Ed.* (2013), 52, 406-409. DOI: 10.1002/anie.201205715. IF: 13.4.

**Abstract:** We report on novel nanosensors for fluorescent imaging of physiological pH values. Features include (a) very small diameters (12 nm); (b) biocompatibility due to the use of a hydrogel kind of material [a commercial poly(ethylene glycol)-co-poly-ethyleneoxide], non-covalent immobilization (based on strong hydrophobic interactions), and (c) lack of toxicity. Such nanosensors, if incorporated into an agar film, enable continuous monitoring of the pH value of bacterial cultures, and thus of their growth.



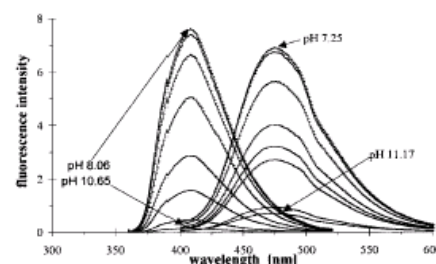
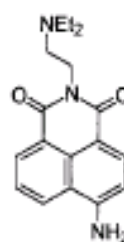
**500. A Nanogel for Ratiometric Fluorescent Sensing of Intracellular pH Values.** H. Peng, J. A. Stolwijk, L. Sun, J. Wegener, O. S. Wolfbeis; *Angew. Chem. Intl. Ed.* (2010), 49, 4246-4249. DOI: 10.1002/anie.200906926. IF: 11.8.

**Abstract:** We are reporting on the first ratiometric fluorescent nanogel (NG) for sensing pH. It can be easily prepared and made pH-responsive via addition of a pH probe and a (ratiometric) FRET system. It has been used to ratiometric imaging of pH inside cells.



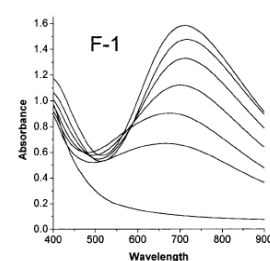
**297. Arenedicarboximide Building Blocks for Fluorescent Photoinduced Electron Transfer pH Sensors Applicable with Different Media and Communication Wavelengths,** L. M. Daffy, A. Prasanna de Silva, H.Q. N. Gunaratne, Ch. Huber, P.L. M. Lynch, T. Werner, O. S. Wolfbeis; *Chem. Eur. J.* 4 (1998) 1810-1815. DOI: 10.1002/(SICI)1521-3765(19980904)4:9<1810::AID-CHEM1810>3.0.CO;2-Y

**Abstract:** N-(aminoalkyl)-4-aminonaphthalene-1,8-dicarboximides (see formula), N-(aminoalkyl)-4-acetamidonaphthalene-1,8-dicarboximides and N,N'-bis(aminoalkyl)-perylene-3,4:9,10-tetracarboxy-diimides show good fluorescent 'off-on' switching in aqueous alcohol solution with protons according to the fluorescent PET sensor design. The excitation maxima are compatible with the blue LED. The probe undergoes substantial fluorescence enhancement with protons when immobilized in a poly(vinyl chloride) (PVC) containing a plasticizer and a borate additive. The fluorophore can be used to sense protons, but also to sense cations such as sodium and potassium if combined with the respective crown ether receptors. All fluorophores may be covalently immobilized on cellulose. The second graph shows the pH dependence of the fluorescence of the N-acetylated probe.



**292. Composite Films of Prussian Blue and N-Substituted Polypyrroles: Fabrication and Application to Optical Determination of pH,** R. Koncki, O. S. Wolfbeis; *Anal. Chem.* 70 (1998) 2544-2550. DOI: 10.1016/S0956-5663(98)00095-5

**Abstract:** A new and simple chemical method for deposition of thin blue films composed of Prussian Blue and N-substituted polypyrroles on non-conductive supports is presented. It is found that only pyrroles which are difficult to polymerize can be used for the preparation of such films. The resulting films were examined by SEM - EDAX, VIS-NIR and IR spectroscopy. The films are stable, thin, and optically transparent. The absorption maxima are at 720 nm and spectral changes can be monitored using LED light sources. The composite films are suitable for optical determination of pH over the pH 5 - 9 range because their abs. depends on pH in the physiological pH range. The films represent an alternative to indicator-based pH sensor materials because they do not require a dye to be immobilized. The pH measurements are highly reproducible, reversible in the physiol. range, and not interfered by ionic strength, alkaline cations, and typical oxidants and reductants. The figure shows the change in the absorption spectra of material F-1 on going from pH 3 (top) to pH 10 (bottom).

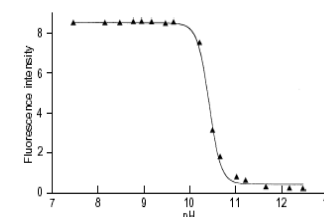
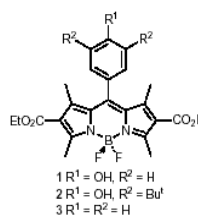


pH-dependence of the absorption spectra of the new materials

**280. Phenol/phenolate-Dependent on/off Switching of the Luminescence of 4,4-Difluoro-4-bora-diaza-indacenes,** T. Gareis, C. Huber, O.S. Wolfbeis and J. Daub; *Chem. Comm.* 1997, 1717-1718. DOI: 10.1039/a703536e

**Abstract:** We describe the protonation-dependent switching of the fluorescence of phenol type derivatives of the bodipy's (a widely used group of fluorescent labels). The lack of emission of the phenolate forms in alkaline solutions is attributed to photo-induced electron transfer (PET) between the phenolate and the bodipy chromophores, resulting in quenching of fluorescence.

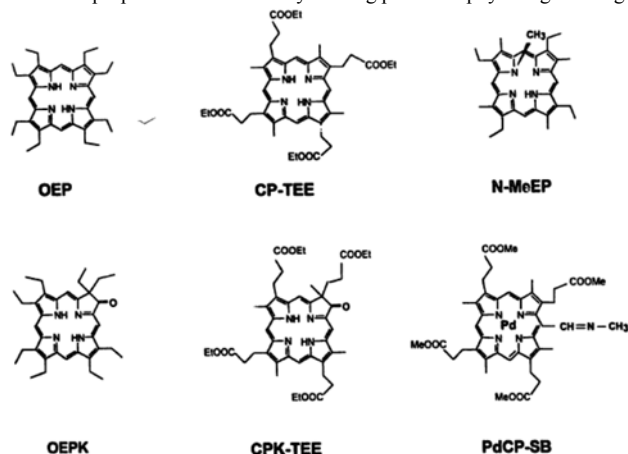
**Figures of merit:** Abs./exc.: 504 nm (chloroform). Em: 522 nm. QY ~0.2 in phenol form. pK<sub>a</sub> values between 9 and 11.



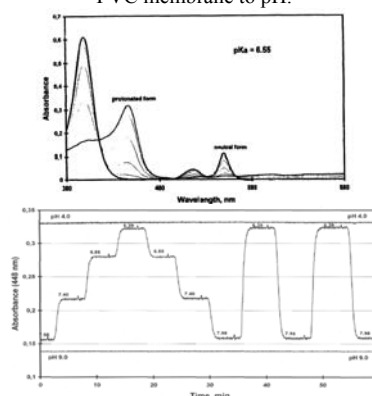


**276. Protonation of Porphyrins in Liquid PVC Membranes: Effects of Anionic Additives and Application to pH-Sensing,** D. B. Papkovsky, G. V. Ponomarev, O. S. Wolfbeis; *J. Photochem. Photobiol., Part A: Chemistry* **104** (1997) 151-158. DOI: 10.1016/S1010-6030(97)04592-9

**Abstract:** We report on a study on the protonation of representative porphyrins, metalloporphyrins, porphyrin-ketones and a Pd-porphyrin Schiff base in aqueous solution and when dissolved in plasticized PVC membranes. The respective protolytic forms were characterized by absorption and emission spectra as well as apparent  $pK_a$  values. It is shown that the protonation of porphyrins dissolved in PVC membranes is much more difficult than in solution, resulting in an extraordinarily large decrease in the apparent  $pK_a$  values which can be as large as 5 pK units when compared to the corresponding data for the porphyrins in solution. In certain cases, no protonation at all occurred within the pH 2-12 range. At the same time, N-MeEP which is much more basic (its intrinsic  $pK$  being 11.2) can be protonated in such membranes into the monocation at weakly acidic pH, but the apparent  $pK_a$  also is lowered by about 6 units. On addition of a tetraphenylborate anion to the PVC membranes, protonation was found to proceed much easier. Both the monocation and dication was identified in case for the porphyrins, while for the porphyrin-ketones direct protonation into dication took place, and N-methyl-etioporphyrin was present as the monocation over the whole pH 2-12 range. Membranes composed of solutions of porphyrin-ketones or the Pd-porphyrin Schiff base in plasticized PVC were identified as being useful for purposes of continuously sensing pH in the physiological range.



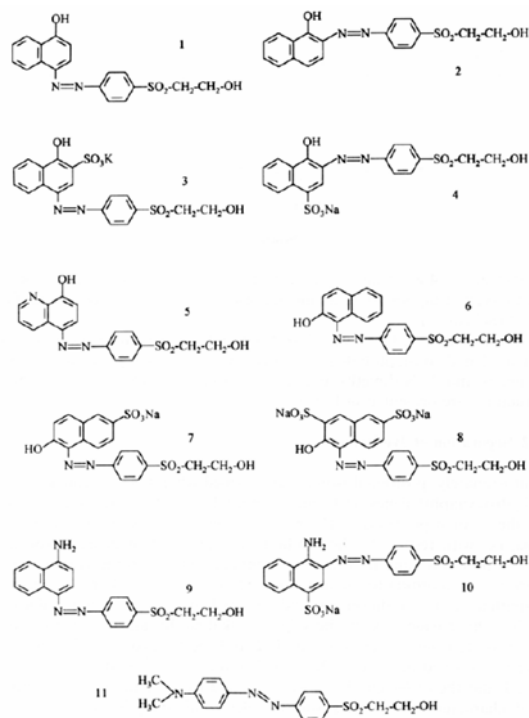
The figures below show typical spectra and the response of a dye-doped plasticized PVC membrane to pH.



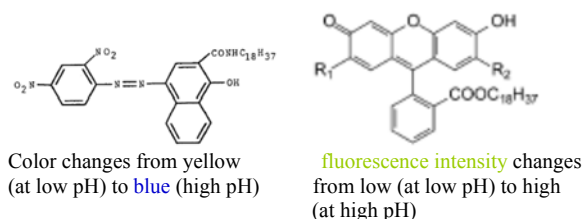
**220. Synthesis of Reactive Vinylsulfonyl Azo Dyes for Application in Optical pH Sensing,** G. J. Mohr, T. Werner, O. S. Wolfbeis, R. Janoschek, *Dyes & Pigments* **24** (1994) 223-240. DOI: 10.1016/0143-7208(94)80011-1

**Abstract:** This work describes the application of a synthon (GM1) capable of forming a variety of reactive azo dyes useful as pH indicators. GM1 possesses two functional groups, namely (a) an amino group which allows diazo coupling to form an indicator chromophore, and (b) a 2-hydroxyethyl-sulphonyl group which, after activation, allows its immobilization on cellulose. GM1 has been diazo coupled with various aromatic phenols and amines to give a variety of pH probes. After conversion of the 2-hydroxyethylsulfonyl group into a reactive vinylsulfonyl group, the dye has been covalently linked to the hydroxy groups of cellulose. We use a novel type of a transparent solid film consisting of a polyester support covered with a thin layer of cellulose acetate which, during immobilization, is converted into cellulose. Cellulose membranes colored with such pH indicating dyes can be applied for optical pH sensing. All dyes are characterized, both in dissolved and immobilized form, in terms of optical properties in the acid and conjugate base form,  $pK_a$  values and indicator properties. Semiempirical AM1 calculations have been performed in order to compute deprotonation energies of three representative dyes, and data were compared with experimental  $pK_a$  values.

The figure shows the chemical structures of the reactive azo dyes 1 to 11.



A related azo dye was also described (H. He et al.; *Anal. Chem.* **65** (1993) 123; DOI: 10.1021/ac00050a006. It is a lipophilic pH probe. Was used in sensors for ions and pH. Color change from yellow to blue. Abs.: 481 nm (yellow) in phenol form (at low pH); 640 nm in alkaline solution. No fluorescence. Another lipophilic pH probe of the fluorescein type is also shown on the right.  $R^1$  and  $R^2$  are hydrogen.  $pK_a$  6.8. A.k.a. McFOE. Ref. B. M. Weidgans et al., *Analyst* **129** (2004) 645. DOI: 10.1039/b404098h. Abs/exc.: 496 nm (log  $\epsilon$  4.52). Em: 523 nm. QY 0.9 at pH > 8;  $\tau$  ~4.5 ns. Another lipophilic pH probe of the fluorescein type has chloro substituents as  $R^1$  and  $R^2$ .  $pK_a$  5.5. Abs/exc.: 502 nm (chloroform). Em: 536 nm. QY 0.9 at pH > 8;  $\tau$  ~4.5 ns. Ref. B. M. Weidgans et al., *Analyst* **129** (2004) 645. DOI: 10.1039/b404098h.

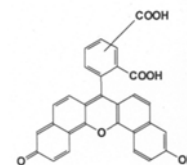




**195. LED-Compatible Fluorosensor for Measurement of Near-Neutral pH Values, O. S. Wolfbeis, T. Werner, N. V. Rodriguez and M. Kessler, *Microchim. Acta* **108**, 133-141 (1992). DOI: 10.1007/BF01242422**

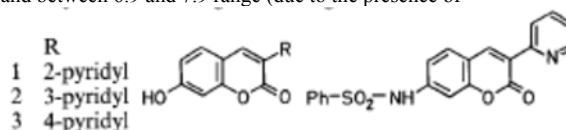
**Abstract:** We report on an optical sensor material suitable for fluorimetric measurement of pH in the 6 - 9 range using a new and LED-compatible fluorescent dye of the naphthofluorescein type. Its base form is blue and has a strong absorption band between 580 and 630 nm that matches the emission wavelengths of conventional yellow or orange LEDs. Two kinds of dye immobilization are reported. The first is based on covalent binding to a cellulosic matrix and the resulting material is intended for use in sensing membranes. The second involves physical entrapment of the dye in a sol-gel matrix which can be used for optical fiber tip coating and in evanescent wave type sensors. Both kinds of sensor materials are studied with respect to dynamic pH ranges, response times, sensitivity toward ion strength, and stability.

**Figures of merit:** Abs (log  $\epsilon$  = 4.6) and exc. at 602 nm (blue) at pH > 8. Em: 670 nm. Abs (log  $\epsilon$  4.3) and exc.: 510 nm (orange) at pH < 7. Em: 572 and 656 nm (2 bands). Naphthofluorescein derived (longwave) pH probe for use in hydrophilic sensor membranes.  $pK_a$  values between 7.4 and 7.6. Was covalently conjugated to aminoethyl cellulose. Probably also a good protein label



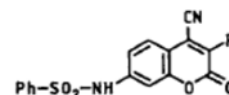
**106. A New Group of Fluorescent pH Indicators for an Extended pH Range, O. S. Wolfbeis, H. Marhold, *Fresenius' Z. Anal. Chem.* **327** (1987) 347-350. DOI: 10.1007/BF00491840**

**Abstract.** We report on the pH versus fluorescence intensity profiles of a series of new pH indicators out of the class of coumarins. They are characterized by two  $pK_a$  values that are located between 3.7 and 4.9 (due to the presence of pyridyl groups) and between 6.9 and 7.9 range (due to the presence of phenol groups and Ph-SO<sub>2</sub>-NH-groups), respectively. The strong change in the intensity of their blue fluorescence with pH allows the determination of pH values over a much wider range (typically 2-9) than with one-step indicators. They are therefore considered to be of potential utility for measurement of pH over the neutral and slightly acidity range which occurs, for instance, in biofluids such as urine or stomach fluids.



**90. Synthesis and Spectral Properties of 7-(N-Arylsulfonyl)-aminocoumarins, a New Class of Fluorescent pH Indicators, O. S. Wolfbeis and J. H. Baustert, *J. Heterocyclic Chem.* **22**, 1215-1218 (1985). DOI: 10.1002/jhet.5570220514**

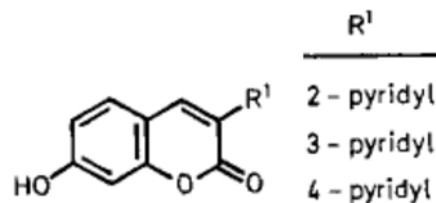
**Abstract.** Coumarins were prep'd. by condensation of benzaldehydes with CH<sub>2</sub>-active compounds, and oxidative cyanation gave the corresponding 4-cyano derivatives. They showed bright blue fluorescence in org. or acidic aq. soln., which was shifted to green in alkaline solution.



**88. Syntheses, Absorption and Fluorescence Spectra of 7-Hydroxy-3-pyridylcoumarins, their Esters, Ethers, and Quaternized Derivatives. O. S. Wolfbeis, H. Marhold, *Chem. Ber.* **118** (1985) 3664-3672. DOI:**

10.1002/cber.198511809

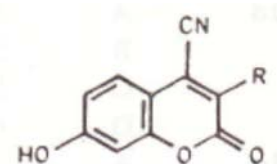
**Abstract.** The title coumarins were prep'd. by condensation of 2-hydroxy-4-methoxybenzaldehyde with pyridylacetic compds. followed by methyl ether cleavage. Its acetates, propionates, and methiodides were also obtained. The absorption and fluorescence spectra in MeOH and water of different pH values were presented, and effects of substituents on spectra and  $pK_a$  values are discussed.



**84. The Unusually Strong Effect of a 4-Cyano Group on the Electronic Spectra and Dissociation Constants of 3-Substituted 7-Hydroxycoumarins, O. S. Wolfbeis, E. Koller, P. Hochmuth, *Bull. Chem. Soc. Jpn.* **58** (1985) 731-734. DOI: 10.1246/bcsj.58.731**

**Abstract:** Synthesis and fluorescence spectra as well as  $pK_a$  values of 7-hydroxycoumarins with electron-withdrawing substituents in positions 3 are described. Introduction of a 4-cyano group is achieved by oxidative cyanation of coumarins using potassium cyanide and elemental bromine. 7-Hydroxycoumarins without a 4-cyano group are useful indicators for measuring physiological pH values due to their intense fluorescences, longwave absorptions and emissions, as well as  $pK_a$  values of around 7.

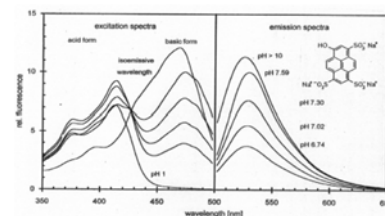
The presence of a 4-cyano group gives rise to a dramatic longwave shift in absorption (30-40 nm in methanol) and emission (55-80 nm). In water solution, the fluorescence maxima are at around 570-600 nm, with excitation maxima between 410 and 510 nm, depending on whether the phenol or phenolate species is excited. For all coumarins under investigation, fluorescence is from the anion form even in the pH 2-7 range. This phenomenon is interpreted in terms of excited state dissociation according to the Förster model. The interpretation is corroborated by calculations of the excited state  $pK_a$  values, which show them to be lower by 4.5-6.4 units than those of the ground state.



**58. A Study on Fluorescent Indicators for Measuring Near-Neutral ("Physiological") pH Values, O. S. Wolfbeis, E. Förlinger, H. Kroneis, and H. Marsoner, *Fresenius' Z. Anal. Chem.* **314**, 119-124 (1983). DOI: 0.1007/BF00482235**



**Abstract.** Fluorescence maxima and  $pK_a$  values of 28 potential indicators are presented in detail, and other data (fluorescence quantum yields, soly., and stability) are given qual. Indicators are divided into groups A and B. Group A compounds exhibit their most long-wave absorption and most intense fluorescence in acidic soln. Group B indicators exhibit their most long-wave absorption and most intense fluorescence in basic soln. As a result of its stability, water solubility, long-wave excitation maximum and large Stokes' shift, HPTS appears to be the pH indicator of choice.

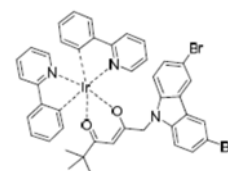


## Section 3. Probes for Temperature

### 497. Dual Sensing of $pO_2$ and Temperature Using a Water-Based and Sprayable Fluorescent Paint. L. H. Fischer, S. M. Borisov, M. Schaeferling, I. Klimant, O. S. Wolfbeis; *Analyst* (2010) 135, 1224-1229. DOI: 10.1039/b927255k.

**Abstract:** Core-shell particles (NPs) composed of a polystyrene core and a poly(vinyl pyrrolidone) shell were dyed with a luminescent platinum(II) porphyrin probe for oxygen. In parallel, microparticles were dyed with a luminescent iridium(II) complex acting as a probe for temperature ( $T$ ). The particles were deposited (by spraying) on a surface to enable continuous imaging of the distribution of oxygen (and thus of barometric pressure) and  $T$ . Unlike in most previous paints of this kind, a binder polymer is not needed and water can be used as a dispersant. This makes the paint environmentally friendly and reduces costs in terms of occupational health and disposal.

Both indicator probes can be excited at 405 nm using LEDs or diode lasers, whilst their emission maxima are spectrally separated by about 130 nm. Thus, two independent optical signals are obtained that allow for fluorescent imaging of barometric pressure (in fact oxygen partial pressure) and of  $T$ , but also to correct the oxygen signal for effects of  $T$ . The paint was calibrated at air pressures ranging from 50 mbar to 2000 mbar and at  $T$ 's between 1 °C and 50 °C. The images show the aluminum foil before and after coating and washing. (A) Before spraying it with the PS/PVP particles; (B) after spraying it with the red paint (dyed with PtTFPP), and (C) after removing the red paint with water.



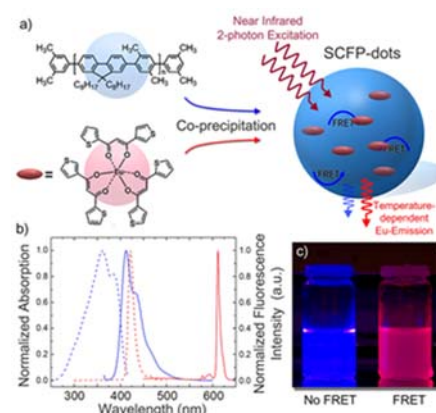
*Figures of merit:* Abs./exc.: 459 nm (log  $\epsilon$  3.45; chloroform). Em: 522 nm.  $\tau$  around 1.6  $\mu$ s

### 596. Two-Photon Excitation Temperature Nanosensors Based on a Conjugated Fluorescent Polymer Doped with a Europium Probe. X.-D.

Wang, R. J. Meier, M. Schaeferling, S. Bange, J. M. Lupton, M. Sperber, J. Wegener, V. Ondrus, U. Beifuss, U. Henne, C. Klein, O. S. Wolfbeis; *Adv. Opt. Mat.* (2016), 4, 1854-1859. DOI: 10.1002/adom.201600601. IF: 6.8.

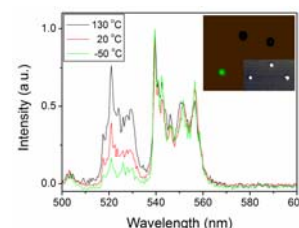
**Abstract.** A strongly fluorescent organic semiconducting polymer doped with a highly temperature dependent fluorescent europium(III) complex was converted into a nanosized material that is capable of optically sensing temperature ( $T$ ) in the range from 0 to 50 °C via two-photon excitation at 720 nm. The nanosensors were prepared from a blue-fluorescent polyfluorene that acts as both a light-harvesting antenna (to capture two-photon energy) and an energy donor in a FRET system. Nanoparticles were obtained by precipitation of the europium(III) complex of 1-(2-thienyl)-3-(3-thienyl)propane-1,3-dione and a semiconducting blue fluorescent polymer. The presence of two emissions (blue and pink; with different dependencies on  $T$ ) enables ratiometric sensing. The photonic energy absorbed by the polymer is transferred to the  $T$ -sensitive red-luminescent europium complex contained in the nanoparticles. The close spatial proximity of the donor and the acceptor warrants efficient FRET. A poly(ethylene glycol)-co-poly(propylene oxide) block copolymer was also added to render the particles biocompatible. We show that  $T$  can be calculated from (a) the intensity of the luminescence of the europium complex, (b) the ratio of the intensities of the red and blue luminescence, or (c) the  $T$ -dependent luminescence lifetime of the Eu(III) complex.

*Figures of merit:* Abs./exc.: 421 nm (log  $\epsilon$  4.6) in water. Em (under 2-photon-excitation at 720 nm): 615 nm.  $\tau$ : 0.2 ms.



### 582. Size Dependence of the Upconverted Luminescence of $NaYF_4:Er,Yb$ Microspheres for Use in Ratiometric Thermometry. B. Dong, R. N. Hua, B. S. Cao, Z. P. Li, Y. Y. He, O. S. Wolfbeis; *PhysChemChemPhys* (2014) 16, 20009-20012. DOI: 10.1039/C4CP01966K. IF: 4.2.

**Abstract:** We report on the size dependence of the upconversion luminescence of temperature ( $T$ )-sensitive particles of the type  $NaYF_4:Er,Yb$  with a size between 0.7 and 2  $\mu$ m that have been prepared by a poly(acrylic acid)-assisted hydrothermal process. It is found that the fluorescence intensity ratio of their green upconversion emissions (with peaks at 521 and 539 nm) is strongly size-dependent at  $T$ 's between 223 and 403 K. If the size of the spheres is increased from 0.7 to 1.6  $\mu$ m, the slope of the sensitivity to  $T$  strongly decreases. This effect is mainly attributed to the larger specific surface area of the smaller spheres where relatively more Er(III) ions are located at the surface. It also shows that sensing  $T$  by this method is prone to error unless particles sizes are well controlled. The Figure shows the upconversion emission spectra at 223 K, 293 K and 403 K.





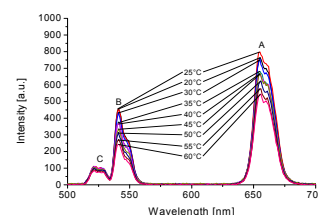
**567. Review: Luminescent Probes and Sensors for Temperature.** X. Wang, R. J. Meier, O. S. Wolfbeis; *Chem. Soc. Rev.* (2013), 42, 7834-7869. DOI: 10.1039/c3cs60102a. Open access. IF: 24.9.

**Abstract:** Temperature ( $T$ ) is the most fundamental parameter in science. Respective sensors also are widely used in daily life. Besides conventional thermometers, optical sensors are considered to be attractive alternatives in sensing and on-line monitoring of  $T$ . This review focuses on all kinds of luminescent probes and sensors for measurement of  $T$  and summarizes the recent progress in their design and application formats. In the introduction, we cover the significance of optical probes for  $T$ , the origin of their  $T$ -dependent spectra, and the various detection modes. This is followed by a survey on (a) molecular probes, (b) nanomaterials, and (c) bulk materials for sensing  $T$ , a discussion of polymeric matrices for immobilizing probes and an overview on the various application formats of  $T$ -sensors. The review closes with a discussion on the prospects, challenges, and new directions in the design of new probes and sensors. 248 references.



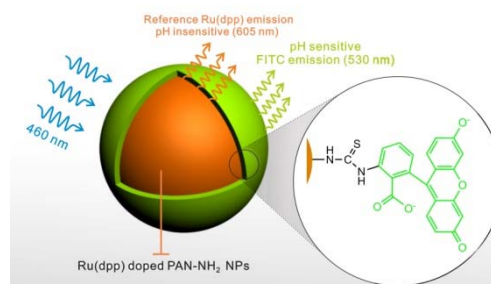
**555. Photon Upconverting Nanoparticles for Luminescent Sensing of Temperature.** A. Sedlmeier, D. E. Achatz, L. H. Fischer, H. H. Gorris, O. S. Wolfbeis; *Nanoscale* (2012), 4, 7090-7096. DOI: 10.1039/c2nr32314a. IF: 5.9.

**Abstract:** Nanoparticles displaying photon upconversion have advantages like the low background fluorescence of biological specimen due to near infrared (NIR) excitation and the presence of two or more emission bands. The ratio of these intensities of the main bands of upconverted emission of hexagonal  $\text{NaYF}_4$  nanoparticles doped with  $\text{Yb}^{3+}$  as the sensitizer and with  $\text{Er}^{3+}$ ,  $\text{Ho}^{3+}$ , or  $\text{Tm}^{3+}$  as the activators yields robust data for the determination of temperature in the “physiological” range (20 – 60°C). Resolutions of  $< \pm 1^\circ\text{C}$  can be achieved with particles consisting of a doped core and an inactive shell.



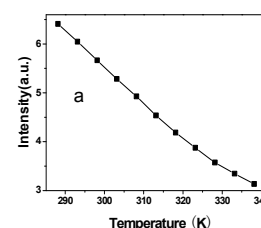
**547. Fluorophore-Doped Polymer Nanomaterial for Referenced Imaging of pH and Temperature with Sub-Micrometer Resolution.** X. Wang, R. J. Meier, O. S. Wolfbeis; *Adv. Funct. Mat.* (2012), 22, 4202-4207. DOI: 10.1002/adfm.201200813. IF: 8.5.

**Abstract:** We report on a new kind of pH and temperature ( $T$ )-sensitive material. It is composed of dye-doped polymer nanoparticles incorporated into a thin film of a polyurethane hydrogel. The new pH/ $T$ -sensitive nanoparticles were obtained by post-staining oxygen-impermeable amino-functionalized polyacrylonitrile nanoparticles with a long-lifetime reference dye. Staining is followed by covalently linking fluorescein isothiocyanate onto the surface of the nanoparticle. The sensor material has distinct features: (a) It enables imaging of pH via time domain dual-lifetime referencing (td-DLR); (b) effects of  $T$  on pH sensing may be compensated for; (c)  $T$  can simultaneously be visualized via rapid lifetime imaging; (d) It offers superior spatial resolution due to the use of nanosized sensor particles.



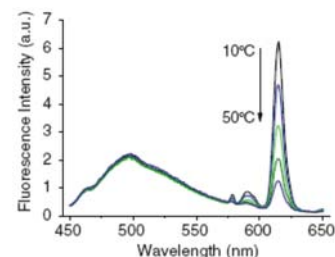
**511. Temperature-Sensitive Luminescent Nanoparticles and Films Based on a Terbium(III) Complex Probe.** L. Sun, J. Yu, H. Peng, J. Z. Zhang, L. Shi, O. S. Wolfbeis; *J. Phys. Chem. C* (2010), 114, 12642-12648. DOI: 10.1021/jp1028323. IF: 4.2.

**Abstract:** The terbium-tris[(2-hydroxy-benzoyl)-2-aminoethyl]amine complex (Tb-THBA) with its high color purity, long luminescence lifetime and high quantum yield has been found to be a viable indicator for optical sensing of temperature ( $T$ ). Both its luminescence intensity and lifetime strongly depend on  $T$  in the range from 15 to 65 °C. When photoexcited at 341 nm, it displays typical  $\text{Tb}^{3+}$  ion emission bands with the strongest peak at 546 nm and a typical decay time of 1.15 ms at 15 °C. The probe is shown to be an excellent for sensing  $T$ , as demonstrated in two kinds of optical sensor membranes.



**509. Ratiometric Fluorescent Nanoparticles for Sensing Temperature.** H. Peng, S. Huang, O. S. Wolfbeis; *J. Nanoparticle Res.* (2010), 12, 2729-2733. DOI: 10.1007/s11051-010-0046-8. IF: 2.5.

**Abstract:** Nanoparticles made from a poly(methyl methacrylate)-co-1,2-bis(trimethoxysilyl)decane composite and containing a red-luminescent europium(III) complex were prepared by the encapsulation-precipitation method. By introducing a green-emitting naphthalimide reference dye, the NPs display both a green and a red fluorescence under single-wavelength excitation. The ratio of fluorescence intensities is highly temperature dependent in the 25 - 45 °C range, with a sensitivity of  $-4.0\%$  per °C. Given their small size (20 – 30 nm) and biocompatibility (due to the presence of an outer layer of silica), such NPs are useful  $T$  sensors for cellular sensing and imaging.

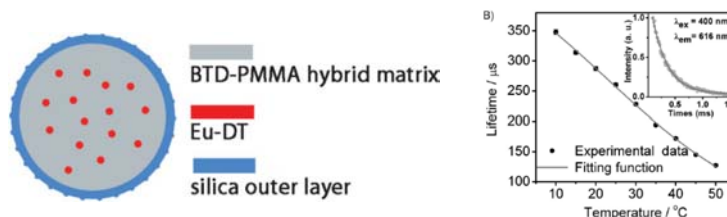




**496. Luminescent Europium(III) Nanoparticles for Sensing and Imaging of Temperature in the Physiological Range.**

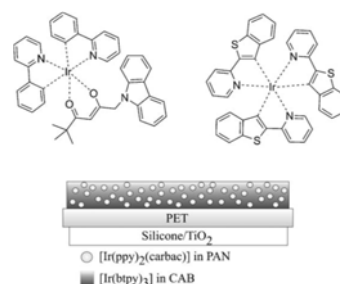
H. Peng, M. I. J. Stich, J. Yu, L. Sun, L. H. Fischer, O. S. Wolfbeis; *Adv. Mat.* (2010), 22, 716-719. DOI: 10.1002/adma.200901614. IF: 8.4.

**Abstract:** Lanthanide-based nano-particles with a diameter of 20–30 nm are introduced for use in luminescent sensing and imaging of physiological temperatures. They are characterized by (i) visible-light photo-excitation, (ii) line-like emission (which facilitates multicolor (dual) sensing), (iii) inert-ness to external perturbors as a result of encapsulation of the europium probe into a biocompatible protective nanoshell, (iv) high photostability, (v) a dynamic range that covers  $T$ 's encountered in medicine, (cellular) biology, and biotechnology, and (vi) good resolution (typically  $\pm 0.3$  °C).

**485. Red and Green Emitting Iridium(III) Complexes for a Dual Barometric and Temperature Sensitive Paint.**

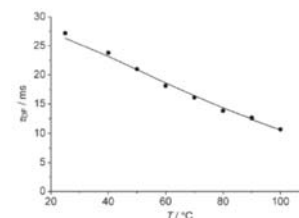
L. H. Fischer, M. I. J. Stich, O. S. Wolfbeis, N. Tian, E. Holder, M. Schaeferling; *Chemistry – Eur. J.* (2009), 15, 10857-10863. DOI: 10.1002/chem.200901511. IF: 5.5.

**Abstract:** A dually luminescent paint for measurement of barometric pressure (BP) and temperature ( $T$ ) is presented. The green-emitting iridium(III) complex Ir-(ppy)(carbac) was applied as a novel probe for  $T$  along with the red-emitting complex Ir-(btpy) which functions as a probe for BP (in fact for oxygen). The two iridium complexes were dissolved in two different polymer materials to achieve optimal responses. The effects of  $T$  on the response of the oxygen probe can be corrected for by simultaneous optical determination of  $T$ . The signals of the probes for  $T$  and BP can be separated by optical filters due to the  $\sim 75$  nm difference in their emission maxima. The dual sensor is applicable to luminescence lifetime imaging of  $T$  and barometric pressure.

**444. An Optical Thermometer Based on the Delayed Fluorescence of C<sub>70</sub>.**

C. Baleizao, S. Nagl, S. M. Borisov, M. Schaeferling, O. S. Wolfbeis, M. N. Berberan-Santos; *Chem. Eur. J.* (2007), 13, 3643-3651. DOI: 10.1002/chem.200601580. IF: 5.0.

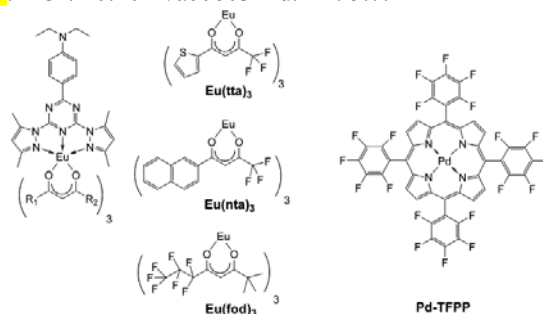
**Abstract:** The thermometer is based on the thermally activated delayed fluorescence of fullerene C<sub>70</sub>. It consists of C<sub>70</sub> molecularly dispersed in various polymer films. In the absence of oxygen and for temp. above 20 °C, the red fluorescence of C<sub>70</sub> in the films is so intense that it is easily perceived by the bare eye. The fluorescence intensity of C<sub>70</sub> increases with temp. by a factor of up to 90, depending on the polymer. This results in a working range from –80 °C to at least 140 °C. Perylene was incorporated as an internal reference in order to enable ratiometric measurements. The sensitivity of the lifetime of the delayed fluorescence to temp. is also high, and results in an even wider working range. The graph shows the temp. dependence of the experimental (circles) and calculated (solid line) lifetimes the delayed fluorescence of C<sub>70</sub> at 700 nm.

**438. Temperature-Sensitive Europium(III) Probes and Their Use for Simultaneous Optical Sensing of Temperature and Oxygen.**

S. M. Borisov, O. S. Wolfbeis; *Anal. Chem.* (2006), 78, 5094-5101. DOI: 10.1021/ac060311d. IF: 5.7.

**Abstract:** Certain luminescent europium(III) complexes (see the Fig.) can act as new probes for optical sensing of temperature ( $T$ ). They can be excited with a 405-nm LED and possess strong brightnesses. The decay times of the probes contained in a poly(vinyl methyl ketone) film and in poly(tert.-butyl styrene) microparticles are highly  $T$ -dependent between 0 and 70 °C. The  $T$ -sensitive microparticles were dispersed, along with oxygen-sensitive microbeads consisting of a Pd(II)porphyrin oxygen probe in a styrene co-polymer, in a thin layer of a hydrogel to give a dually-sensing material that can be photoexcited by a single light source. The two emissions can be separated by appropriate optical filters. The response to oxygen and  $T$  is described by 3D plots, and unbiased values can be obtained for  $T$  and oxygen, respectively, from the two luminescence signals if refined in an iteration step. The sensing scheme is intended for use in  $T$ -compensated sensing of oxygen, in contactless sensing of oxygen and  $T$  in (micro)biological and medical applications, in high resolution oxygen profiling, and for simultaneous imaging of air pressure and  $T$  in wind tunnels.

**Figures of merit:** Abs. and exc. of the Eu(III) complexes: near 402 nm ( $\log \epsilon = 4.86$ , in toluene). Em: 616 nm. Decay time: 0.8 ms at 0 °C, and around 0.3 ms at 50 °C. Range: 0 to 70 °C. Abs. and exc. of the Pd(II) complex: Abs. at 406 nm ( $\epsilon = 192,000$  M<sup>-1</sup> cm<sup>-1</sup>) in toluene. Em: 670 nm.

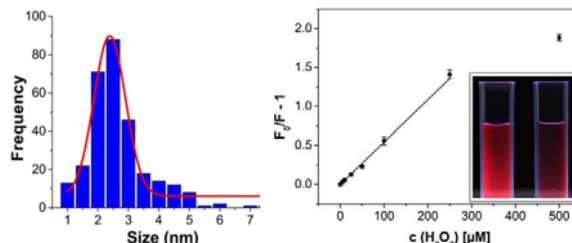




## Section 4. Probes for Hydrogen Peroxide

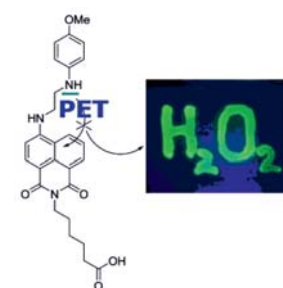
### 597. Europium-doped GdVO<sub>4</sub> Nanocrystals as a Luminescent Probe for Hydrogen Peroxide and for Enzymatic Sensing of Glucose. V. Muhr, M. Buchner, T. Hirsch, D. J. Jovanović, S. D. Dolić, M. D. Dramićanin, O. S. Wolfbeis; *Sensors Actuat., B: Chemical* (2017), 241, 349-356. DOI: 10.1016/j.snb.2016.10.090. IF: 6.4.

**Abstract.** The authors describe the preparation of Eu<sup>3+</sup>-doped GdVO<sub>4</sub> nanocrystals (NCs) by precipitation of the Gd<sup>3+</sup>(Eu<sup>3+</sup>)-citrate complex which was then converted to the respective vanadate by dialysis. The fractions of Eu<sup>3+</sup> ranged from 5 to 100 mol%. The NCs were characterized by XRD, TEM, ICP-OES and dynamic light scattering which revealed that they possess superior colloidal stability in aqueous solutions in that no precipitation can be observed even after several months. The NCs display red and largely red-shifted fluorescence (peaking at 618 nm) on photoexcitation at around 300 nm. Fluorescence is strongly quenched by hydrogen peroxide. It is also shown that the fraction of doping with Eu<sup>3+</sup> strongly affects quenchability. Most efficient quenching by H<sub>2</sub>O<sub>2</sub> is observed if the NCs are doped with 50% of Eu<sup>3+</sup>. The findings were exploited to develop a fluorometric assay for H<sub>2</sub>O<sub>2</sub> that works in the 5 to 250 μM concentration range, with a limit of detection as low as 1.6 μM (at a signal-to-noise ratio of 3). The probe was further employed to design a highly sensitive enzymatic assay for glucose via measurement of the quantity of H<sub>2</sub>O<sub>2</sub> formed as a result of the catalytic action of glucose oxidase.



### 541. A New Fluorescent PET Probe for Hydrogen Peroxide, and its Use in Enzymatic Assays for L-Lactate and D-Glucose. D. B. M. Groegel, M. Link, A. Duerkop, O. S. Wolfbeis; *ChemBioChem* (2011), 12, 2779-2785. DOI: 10.1002/cbic.201100561. IF 3.9.

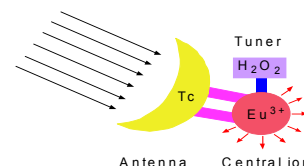
**Abstract:** The probe is based on the yellow fluorophore 4-amino-1,8-naphthalimide that is coupled to p-anisidine (as a redox-active group) to form a probe that is based on photoinduced electron transfer (PET). The preparation of the probe (to which we refer as HP Green) was accomplished in four steps. Its fluorescence is independent of pH in the physiological range and quenched due to a PET process that occurs between the p-anisidine redox moiety and the naphthalimide luminophore. If the p-anisidine group is oxidized by HP, PET is suppressed and fluorescence intensity is strongly increased. Addition of horseradish peroxidase (HRP) enhances the oxidation of HP Green and further improves the detection limit of HP. The use of HRP and HP Green enables the determination of HP with a limit of detection (LOD) as low as 64 nM. HP Green also enables sensitive enzymatic assays of L-lactate and D-glucose using the respective oxidases.



### 427. Nonenzymatic Direct Assay of Hydrogen Peroxide at Neutral pH Using the Eu<sub>3</sub>Tc Fluorescent Probe. A. Duerkop, O. S. Wolfbeis; *J. Fluoresc.* 2005, 15, 755-761. DOI: 10.1007/s10895-005-2984-6. IF: 2.6.

**Abstract:** A detailed study is presented on the use of an easily accessible probe (the europium–tetracycline 3:1 complex; referred to as Eu<sub>3</sub>Tc) for determination of hydrogen peroxide (HP). Eu<sub>3</sub>Tc undergoes a 15-fold increase in luminescence intensity on exposure to an excess of HP. Data are given on the time dependence of the reaction, on the pH dependence of the absorption and emission spectra. HP can be quantified in aqueous solution of pH 6.9 over a 2–400 μM concentration range with a limit of detection of 960 nM. The assay is validated using standard additions, and mean recoveries are found to be between 97.0 and 101.8 %. Species that interfere in concentrations below 1 mM include phosphate, copper(II), fluoride and citrate. The method is critically assessed with respect to other optical methods for determination of HP.

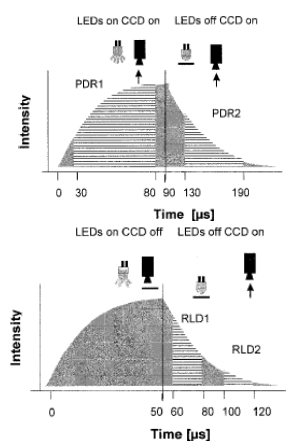
**Figures of merit:** Abs. or exc.: 401 nm (log ε 4.2); Em: 616 nm; QY 0.003 in absence of H<sub>2</sub>O<sub>2</sub>, but 0.04 in its presence. Decay time near 8.7 μs. This is the Eu(III) 3:1 complex with tetracycline.



### 392. Time-Resolved Luminescence Imaging of Hydrogen Peroxide Using Europium-Tetracycline Sensor Membranes in a Microwell Format, M. Schaeferling, M. Wu, J. Enderlein, H. Bauer, O. S. Wolfbeis; *Appl. Spectrosc.* 57 (2003) 1386-1392. DOI: 10.1366/000370203322554554. IF: 1.9.

**Abstract:** We demonstrate an optical imaging scheme for hydrogen peroxide in a microwell-based format using the europium(III) tetracycline complex as the fluorescent probe, which is incorporated into a poly(acrylonitrile)-co-poly(acrylamide) polymer matrix. The resulting sensor membranes are integrated into a 96-microwell plate. Hydrogen peroxide can be visualized by means of time-resolved imaging. The imaging system consists of a fast, gated CCD camera and a pulsed array of 96 LEDs. Fluorescence lifetime images were acquired by both rapid lifetime detection and phase delay rationing, and compared with intensity-based methods with respect to sensitivity and dynamic range. The response time of the sensor is comparatively high, typically in the range of 10 to 20 min, but the response is reversible. The largest signal changes are observed at pH 6.5–7.5. Below is a schematic representation of the time gates in the PDR imaging method (left), and in the RLD imaging method (right). In the PDR scheme, the luminescence is measured first in the excitation period (PDR1), and then in the emission period (PDR2). In the RLD scheme, both time gates (RLD1 and RLD2) are detected during the emission period.

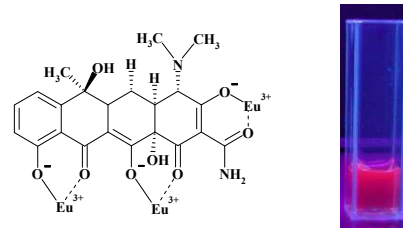
**Figures of merit:** Abs. or exc.: 401 nm (log ε 4.2); Em: 616 nm; QY 0.003 in absence of H<sub>2</sub>O<sub>2</sub>, but 0.04 in its presence; Decay time near 8.7 μs. This is the Eu(III) 3:1 complex with tetracycline.





**373. Europium Ion-Based Luminescent Sensing Probe for Hydrogen Peroxide,** O. S. Wolfbeis, A. Duerkop, M. Wu and Z. Lin; *Angew. Chem.* **114** (2002); 4681-4684; *Intl. Ed. Engl.* **41** (2002) 4495-4498. DOI: 10.1002/1521-3773(20021202)41:23<4495::AID-ANIE4495>3.0.CO;2-I. IF: 10.3.

**Abstract:** The fluorescence of the Eu(III) complex with tetracycline (EuTc) undergoes a 15-fold increase in intensity and a change in its decay time if exposed to hydrogen peroxide. Thus, EuTc can act as a molecular probe for H<sub>2</sub>O<sub>2</sub> (HP). This is exploited (a), to detect HP in trace quantities (< 1 ppm); (b) to detect glucose (via formation of HP by glucose oxidase); (c) the determination of the activity of oxidases; and (d) the detection of enzyme inhibitors. The probe is best excited at 400-405 nm (and thus compatible with the 405-nm diode laser), displays a narrow emission band peaking at 616 nm, and has a QY of 4%. The decay profile of EuTc is composed of 3 main components, with decay times of ca. 9, 30, and 170 microseconds, respectively. The first picture shows the assumed chemical structure of EuTc, and the second the pink (616-nm) line-like "fluorescence" that can be observed on addition of hydrogen peroxide to a virtually non-fluorescent solution of the EuTc complex.

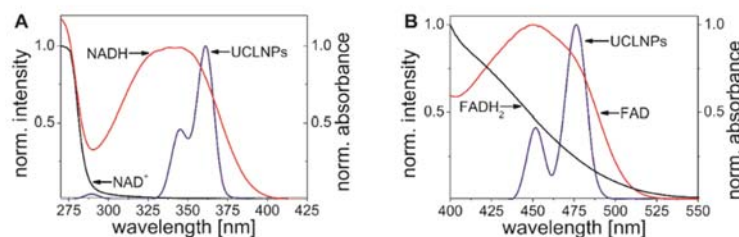


**Figures of merit:** Abs. or exc.: 401 nm (log  $\epsilon$  4.2); Em: 616 nm; QY 0.003 in absence of H<sub>2</sub>O<sub>2</sub>; but 0.04 in its presence; Decay time near 8.7  $\mu$ s;  $\tau_2$  30  $\mu$ s. This is the Eu(III) 3:1 complex with tetracycline.

## Section 5. Probes for Enzyme Activity, Inhibition Assays, and Enzymatic Assays of Substrates

**583. Spectrally Matched Upconverting Luminescent Nanoparticles for Monitoring Enzymatic Reactions.** S. Wilhelm, M. del Barrio, J. Heiland, S. F. Himmelstoss, J. Galbán, O. S. Wolfbeis, T. Hirsch; *ACS Appl. Mat. Interf.* (2014), 6, 15427-15433. DOI: 10.1021/am5038643. IF: 5.0.

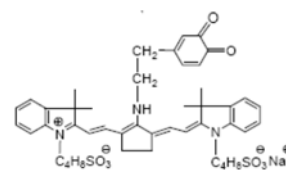
**Abstract:** We report on upconverting luminescent nanoparticles (UCLNPs) that are spectrally tuned such that their emission matches the absorption bands of the two most important species associated with enzymatic redox reactions. The core-shell UCLNPs consist of a hexagonal NaYF<sub>4</sub> core doped with Yb(III) and Tm(III) ions, and a shell of undoped hexagonal NaYF<sub>4</sub>. Upon 980-nm excitation, they display emission bands peaking at 360 nm and 475 nm which is a perfect match to the absorption bands of the enzyme cosubstrate NADH (360 nm) and the coenzyme FAD (475 nm), respectively. By exploiting these spectral overlaps, we have designed fluorescent detection schemes for NADH and FAD that are based on the modulation of the emission intensities of UCLNPs by FAD and NADH via an inner filter effect. The Figures below show the normalized upconversion luminescence spectra of hydrophilic hexagonal NaYF<sub>4</sub>:Yb,Tm@NaYF<sub>4</sub> core-shell particles dispersed in MES buffer, and the overlap with the absorption bands of NADH (left) and FAD (right)



**Figures of merit:** Exc: 980 nm (water). Em: 360 and 475 nm.  $\tau$ : around 100  $\mu$ s. The UCLNPs display emission bands peaking at 360 nm (purple; screened off by NADH) and 475 nm (green; screened off by FAD).

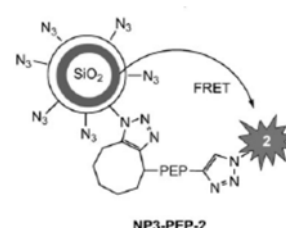
**502. A Near-Infrared Fluorescent Probe for Monitoring Tyrosinase Activity.** X. Li, W. Shi, S. Chen, J. Jia, H. Ma, O. S. Wolfbeis; *Chem. Comm.* (2010), 2560-2562. DOI: 10.1039/c001225d. IF: 5.5.

**Abstract:** We report on the first NIR fluorescent probe for monitoring tyrosinase activity. Upon reaction with tyrosinase, the tyramine moiety of the probe was oxidized into o-quinone, which leads to quenching via intramolecular electron transfer from the cyanine skeleton to the quinone unit.



**491. Probing the Activity of Matrix Metalloproteinase II Using a Sequentially Click-Labeled Silica Nanoparticle FRET Probe.** D. E. Achatz, G. Mezö, P. Kele, O. S. Wolfbeis; *ChemBioChem* (2009), 10, 2316-1320. DOI:

10.1002/cbic.200900261. IF: 3.3. **Abstract:** Fluorescent core-shell silica nanoparticles (SiNPs) bearing a fluorescently labeled substrate for the tumor marker protease MMP-2 were prepared. FRET from the SiNP to the label is observed but suppressed once the substrate is hydrolyzed by the enzyme. The reaction rate is a direct parameter for determining the activity of MMP-2.



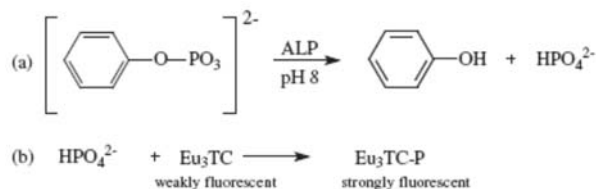
**460. Time-Resolved Fluorescence-Based Assay for the Determination of Alkaline Phosphatase Activity, and Application to the Screening of its Inhibitors.** P. Schrenkhammer, I. C. Rosnizeck, A. Duerkop, O. S. Wolfbeis, M. Schaeferling, J. Biomol. Screen. (2008), 13, 9-16. DOI: 10.1177/1087057107312031. IF: 2.8.

**Abstract:** A single-step end point method is presented for detn. of the activity of the enzyme alk. phosphatase (ALP) using the effect of enhancement of



fluorescence of the easily accessible europium(III)-tetracycline 3:1 complex (EuTC). Its luminescence, peaking at 616 nm if excited at 405 nm, is enhanced by a factor of 2.5 in the presence of phosphate. Phenyl phosphate was used as a substrate that is enzymically hydrolyzed to form phenol and phosphate. The latter coordinates to EuTC and enhances its luminescence intensity as a result of the displacement of water from the inner coordination sphere of the central metal. The assay is performed in a time-resolved (gated) mode, which is shown to yield larger signal changes than steady-state measurement of fluorescence. The limit of detection for ALP is 4 mmol/L. Based on this scheme, a model assay for theophylline as inhibitor for ALP was developed with a linear range from 14 to 68 mmol/L of theophylline.

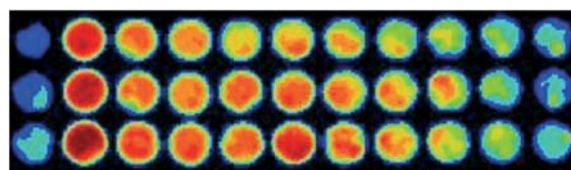
*Figures of merit:* Abs. or exc.: 401 nm (log  $\epsilon$  4.2); Em: 616 nm; QY 0.003 in absence of H<sub>2</sub>O<sub>2</sub>, but 0.04 in its presence. Decay time near 8.7  $\mu$ s;  $\tau_2$  30  $\mu$ s. This is the Eu(III) 3:1 complex with tetracycline.



#### 431. Novel Method for Time-Resolved Fluorometric Determination and Imaging of the Activity of Peroxidase, and its Application to Enzyme-Linked Immunosorbent Assays, Z. Lin, M. Wu, O. S. Wolfbeis, M. Schaeferling; *Chem. – Eur. J.* (2006), 12, 2730-2738. DOI: 10.1002/chem.200500884. IF: 5.0.

**Abstract:** A new format for enzyme-linked immunosorbent assays (ELISA) is described, using the europium(III) tetracycline complex [Eu(Tc), 3:1] as a fluorescent probe for hydrogen peroxide (HP). [Eu(Tc)] forms a strongly fluorescent complex with HP, and the peroxidase-catalyzed decomposition of the system [Eu(Tc)-HP] can be monitored via the decrease in fluorescence due to the formation of the weakly fluorescent [Eu(Tc)]. Due to this effect, the europium probe can be used to detect the presence of peroxidases linked to antibodies. Furthermore, the fluorescence decay time of [Eu(Tc)-HP] is in the

range of 60  $\mu$ s, which enables the application of time-resolved detection methods. These show superior properties compared to intensity-based techniques due to better elimination of background signals. The time-resolved (“gated”) fluorescence assays cover a dynamic range from 0.1 – 8 ng/mL for the quantitation of bovine IgG by peroxidase-labeled anti-bovine IgG in a sandwich-type ELISA. Multiplexed samples can alternatively be visualized directly and evaluated quantitatively by means of fluorescent imaging with the help of an array of light-emitting diodes (LEDs) and a CCD camera. The figure shows a typical array of images as obtained by time-resolved imaging of microwell spots (sandwich assay format).

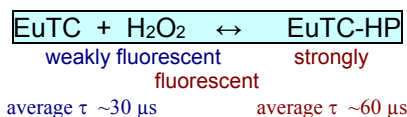


*Figures of merit:* Abs. or exc.: 401 nm (log  $\epsilon$  4.2); Em: 616 nm; QY 0.003 in absence of H<sub>2</sub>O<sub>2</sub>; but 0.04 in its presence. Decay time around 8.7  $\mu$ s.

#### 412. Fluorescence Imaging of the Activity of Glucose Oxidase Using a Hydrogen Peroxide Sensitive Europium Probe, M. Wu, Z. Lin, M. Schaeferling, A. Duerkop, O. S. Wolfbeis; *Anal. Biochem.* 2005, 340, 66-73. DOI: 10.1016/j.ab.2005.01.050. IF: 3.0.

**Abstract:** A method for optical imaging of the activity of glucose oxidase (GOx) using a fluorescent europium(III) tetracycline probe (EuTC) for hydrogen peroxide is presented. A decay time in the microsecond range and the large Stokes' shift of 210 nm of the probe facilitate intensity-based, time-resolved, and decay-time-based imaging of glucose oxidase. Four methods for imaging the activity of GOx were compared, and rapid lifetime determination imaging was found to be the best in giving a linear range from 0.32 to 2.7 mUnit/mL. The detection limit is 1.7 ng/mL. Fluorescent imaging of the activity of GOx is considered to be a useful tool for GOx-based immunoassays with potential for high-throughput screening, immobilization studies, and biosensor array technologies.

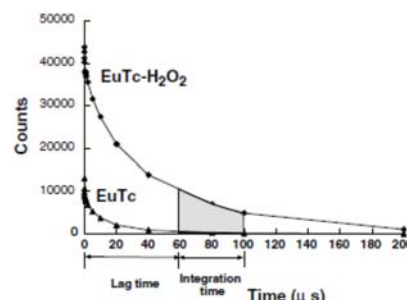
*Figures of merit:* Abs. or exc.: 401 nm (log  $\epsilon$  4.2); Em: 616 nm; QY 0.003 in absence of H<sub>2</sub>O<sub>2</sub>; but 0.04 in its presence; Decay time near 8.7  $\mu$ s;  $\tau_2$  30  $\mu$ s. This is the Eu(III) 3:1 complex with tetracycline.



#### 405. Time-Resolved Enzymatic Determination of Glucose Using a Fluorescent Europium Probe for Hydrogen Peroxide, M. Wu, Z. Lin, A. Duerkop, O. S. Wolfbeis; *Anal. Bioanal. Chem.* (2004), 380, 619-626. DOI: 10.1007/s00216-004-2785-9. IF: 2.9.

**Abstract:** An enzymatic assay for glucose based on the use of the fluorescent probe for hydrogen peroxide, europium(III) tetracycline (EuTc), is described. The weakly fluorescent EuTc and enzymatically generated H<sub>2</sub>O<sub>2</sub> form a strongly fluorescent complex (EuTc-H<sub>2</sub>O<sub>2</sub>) whose fluorescence decay profile is significantly different. Since the decay time of EuTc-H<sub>2</sub>O<sub>2</sub> is in the microseconds time domain, fluorescence can be detected in the time-resolved mode, thus enabling substantial reduction of background fluorescence. The scheme represents the first H<sub>2</sub>O<sub>2</sub>-based time-resolved fluorescence assay for glucose not requiring the presence of a peroxidase. The time-resolved assay (with a delay time of 60  $\mu$ s and using endpoint detection) enables glucose to be determined at levels as low as 2.2  $\mu$ M, with a dynamic range of 2.2–100  $\mu$ M. The method also was adapted to a kinetic assay in order to cover higher glucose levels (mM range). The latter was validated by analyzing spiked serum samples and gave a good linear relationship for glucose levels from 2.5 to 55 mM. Noteworthy features of the assay include easy accessibility of the probe, large Stokes' shift, a line-like fluorescence peaking at 616 nm, stability towards oxygen, a working pH of approximately 7, and its suitability for both kinetic and endpoint determination.

*Figures of merit:* Abs. or exc.: 401 nm (log  $\epsilon$  4.2); Em: 616 nm; QY 0.003 in absence of H<sub>2</sub>O<sub>2</sub>, but 0.04 in its presence. Decay time near 8.7  $\mu$ s;  $\tau_2$  30  $\mu$ s. This is the Eu(III) 3:1 complex with tetracycline.

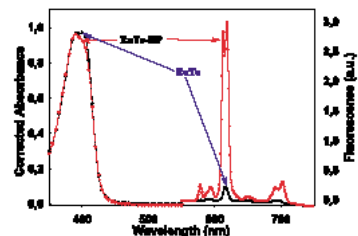


#### 383. Determination of the Activity of Catalase Using a Europium(III)-Tetracycline-Derived Fluorescent Substrate, M. Wu, Z. Lin, O. S. Wolfbeis; *Anal. Biochem.* 320 (2003) 129-135. DOI: 10.1016/S0003-2697(03)00356-7. IF: 3.0.



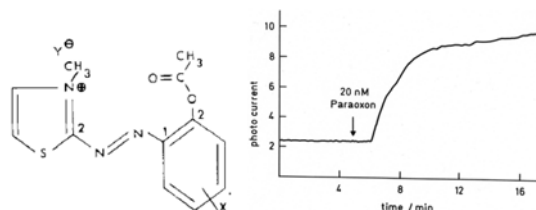
**Abstract:** A one-step method is described for the fluorometric determination of the activity of the enzyme catalase (EC 1.11.1.6.), based on the finding that H<sub>2</sub>O<sub>2</sub> in the Eu<sup>3+</sup>-tetracycline-hydrogen peroxide system is consumed by catalase. This is accompanied by a large decrease in both fluorescence intensity (see the figure) and decay time. The limit of detection (LOD) for catalase at 30 °C for a 10-min kinetic assay is 1.0 unit/mL. At an It is a one-step, simple, and sensitive method suitable for both continuous kinetic and one-point detections, does not require the addition of other substrates, and works best at neutral pH (with an optimum at pH 6.9). The reagent has the typical spectral features of a europium-ligand complex including a 219-nm Stokes shift, a line-like emission (centered at 616 nm), and a decay time in the microsecond domain. The EuTc-HP complex also is the first europium-based probe that is compatible with the 405-nm diode laser.

**Figures of merit:** Abs. or exc.: 401 nm (log  $\epsilon$  4.2); Em: 616 nm; QY 0.003 in absence of H<sub>2</sub>O<sub>2</sub>, but 0.04 in its presence. Decay time near 8.7  $\mu$ s. This is the Eu(III) 3:1 complex with tetracycline.



## 208. Fiber Optic Remote Detection of Pesticides and Related Inhibitors of the Enzyme Acetylcholinesterase, W. Trettnak, F. Reininger, E. Zinterl, O. S. Wolfbeis; *Sensors Actuators B11*, 87-93 (1993). DOI: 10.1016/0925-4005(93)85242-3

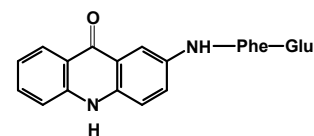
**Abstract:** A method for remote detection of inhibitors of the enzyme AChE is presented that makes use of a fiber optic photometer based exclusively on solid-state opto-electronic components including light-emitting diodes and photodiodes. The method employs a yellow synthetic enzyme substrate (see formula) which is hydrolyzed by the enzyme to give a blue product. In the presence of an inhibitor, the rate of the formation of this blue product is reduced. The resulting signal change is detected via fiber optics over time and may serve as an alarm.



## 133. Fluorometric Continuous Kinetic Assay of $\alpha$ -Chymotrypsin Using New Substrates Possessing Longwave Excitation and Emission Maxima, J. Baustert, O. S. Wolfbeis, R. Moser and E. Koller, *Anal. Biochem.* **171**, 393-397 (1988). DOI: 10.1016/0003-2697(88)90503-9

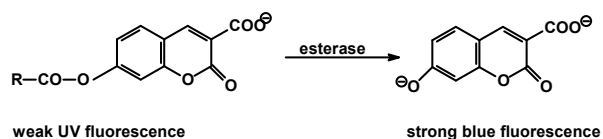
**Abstract.** A direct and continuous kinetic method for the fluorometric detn. of alpha-chymotrypsin and trypsin is described, and 2-aminoacridone (2-AA) is introduced as a new fluorophore in anal. biochem. N-Succinyl- and N-glutarylphenylalanine were coupled to 2-AA via a peptide bond and the resulting fluorogenic substrates were cleaved by the 2 enzymes. Since the substrate and product of hydrolysis have quite different spectral properties, the increase in the long-wave fluorescence of 2-AA (measured at 570 nm under 450-nm excitation) is a parameter for enzyme activity. Chymotrypsin (0.5  $\mu$ g/mL) and trypsin (0.1  $\mu$ g/mL) were detectable in a 3-min assay using the new substrates. Several other fluorogenic peptides are also described.

**Figures of merit:** Abs: 450 nm (log  $\epsilon$  4.2). Em: 570 nm. QY 0.65.



## 124. A Sensitive Kinetic Assay of Serum Albumins Based on Their Enzyme-like Hydrolytic Activity Using a New Chromogenic and Fluorogenic Substrate, A. Gürakar & O.S. Wolfbeis; *Clin. Chim. Acta* **172**, 35-46 (1988). DOI: 10.1016/0009-8981(88)90118-0

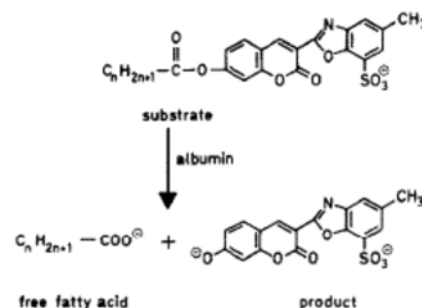
**Abstract.** A new albumin assay, based on the unusual enzyme-like activity of the protein that promotes hydrolysis of ester bonds in fatty acid arylesters was designed for clin. routine use. The substrate introduced shows improved anal. wavelengths and is suitable for both photometric and fluorometric assays. Experiments have been performed with a conventional photometer, a fluorometer, and an automated analyzer. Detection limits are as low as 10  $\mu$ g/mL photometrically and 20 ng/mL fluorometrically. The method provides a sensitive quantitative determination of even minute amounts. of albumin in liquid solution, and a simple semiquantitative test may be performed by fixing the dye on a test strip which then is immersed into a sample solution and observing the development of yellow color intensity.



## 109. The Effect of Fatty Acid Chain Length on the Rate of Arylesterase Hydrolysis by Various Albumins, O. S. Wolfbeis and A. Gürakar, *Clin. Chim. Acta* **164**, 329-337 (1987). DOI: 10.1016/0009-8981(87)90308-1

**Abstract.** A series of synthetic chromogenic and fluorogenic substrates for monitoring the aryl esterase-like activity of albumins from various sources was studied. Except for ovalbumin, all displayed enzyme-like activity. The acetate, butyrate, caprylate, laurate, and palmitate esters of a coumarin dye were found to be efficiently hydrolyzed within the pH range 8.8 - 9.8, with the non-enzymic rate being highest for acetate and lowest for laurate. The latter was considered to be the substrate of choice because it was cleaved most quickly by the proteins tested. A considerable increase in hydrolytic activity was obsd. on addn. of detergents, but not of Ca<sup>2+</sup> and Mg<sup>2+</sup>, whereas addn. of lauric acid to bovine serum album resulted in a 30% decrease in its activity. The results were interpreted in terms of the well-known affinity of albumins for long-chain fatty acids and provide the basis for a sensitive determination of small amts. of albumins.

**Figures of merit:** Abs. or exc.: 378 nm; Em: 455 nm; QY 0.7 in pH 8 solution after hydrolysis to the phenol (anion). Also hydrolyzed by various albumins: O. S. Wolfbeis et al; *Clin. Chim. Acta* **164** (1987) 329. DOI: 10.1016/0009-8981(87)90308-1. More longwave substrates also described.

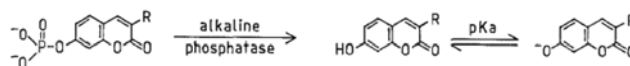




**91. Photometric and Fluorimetric Assay of Alkaline Phosphatase with New Coumarin-Derived Substrates, O. S. Wolfbeis and E. Koller, *Microchim. Acta* **85** (1985) 389-395. DOI: 10.1007/BF01201534**

**Abstract.** Two 7-hydroxycoumarin derivs. were tested as substrates for the detn. of alkaline phosphatase. The optimum pH for assays with both substrates was 9.5. Rates of hydrolysis of the substrates were relatively high (1.5 - 1.8 nmol/min) when detd. by either spectro-photometry or fluorometry, although the sensitivity of the fluorometric assay was higher ( $1 \times 10^{-5}$  units/mL, vs.  $5 \times 10^{-4}$  units/mL for the photometric assay).

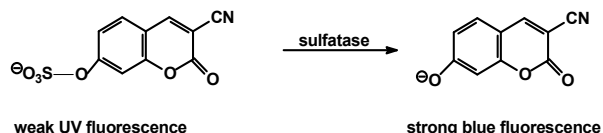
**Figures of merit:** Abs. and exc.: 378 nm. Em: 455 nm; QY 0.7 in pH 8 solution after hydrolysis to the phenol (anion).



**87. Continuous Kinetic Assay of Arylsulfatases with New Chromogenic and Fluorogenic Substrates, E. Koller, O.S. Wolfbeis; *Anal. Chim. Acta* **170**, 73-80 (1985). DOI: 10.1016/S0003-2670(00)81727-4**

**Abstract.** Arylsulfatases can be detd., even in weakly acidic soln., by a direct and continuous kinetic method using new coumarin-derived sulfates as substrates. After enzymic hydrolysis, the substrate dissociates to form intensely colored and strongly fluorescent phenolates, with absorption maxima from 383 - 497 nm and fluorescence emission maxima of 470 - 577 nm.

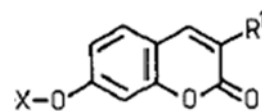
**Figures of merit:** Abs. and exc.: 378 nm. Em: 455 nm; QY 0.7 in pH 8 solution after hydrolysis to the phenol (anion).



**83. Synthesis and Spectral Properties of Longwave Absorbing and Fluorescing Substrates for the Direct Kinetic Assay of Carboxylesterases, Phosphatases, and Sulfatases, E. Koller, O. S. Wolfbeis; *Monatsh. Chem.* **116** (1985) 65-75. DOI: 10.1007/BF00798280**

**Abstract.** Syntheses, absorption and fluorescence properties for a series of new enzyme substrates are described, which are derived from 7-hydroxycoumarins possessing electron-withdrawing substituents in position 3 ( $= R^1$ ), for example  $-\text{COOH}$ ,  $-\text{CN}$ ,  $-2\text{-benzoxazolyl}$ , or  $-\text{benzothiazolyl}$ . The new substrates are advantageous over existing ones in that they exhibit longwave absorption and fluorescence maxima as well as large Stokes' shifts. In addition, their  $\text{pK}_a$  values, which are usually between 6.0 and 7.0, allow the direct and continuous kinetic assay of hydrolases such as esterases, phosphatases, and sulfatases.

**Figures of merit:** Abs. and exc.: 378 nm. Em: 455 nm; QY 0.7 in pH 8 solution after hydrolysis to the phenol (anion).

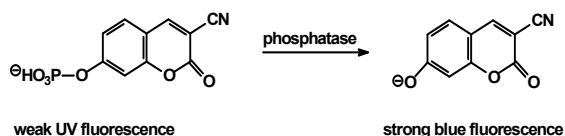


X = fatty acid, sulfate, or phosphate

**79. Photometric and Fluorometric Continuous Kinetic Assay of Acid Phosphatases with New Substrates Possessing Longwave Absorption and Emission Maxima, E. Koller & O.S. Wolfbeis; *Anal. Biochem.* **143**, 146-151 (1984). DOI: 10.1016/0003-2697(84)90569-4**

**Abstract.** A direct and continuous kinetic method for the photometric and fluorometric detn. of various acid phosphatases is described. It is based on new coumarin-derived phosphates, which after enzymic hydrolysis undergo disson. to form intensely colored and strongly fluorescent phenolate anions. The latter have absorption max. of 385- 505 nm, and fluorescence max. of 470-595 nm. The new substrates were compared with respect to their rate of enzymic hydrolysis, optimum pH, and detection limits of acid phosphatase from potato and wheat germ. Detection limits of 1 milli-unit/mL were found by photometry, and as low as  $6 \mu\text{-units/mL}$  by fluorometry.

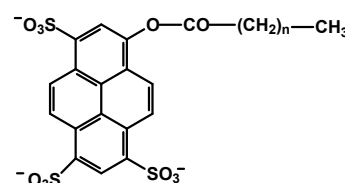
**Figures of merit:** Abs. and exc.: 378 nm. Em: 455 nm; QY 0.7 in pH 8 solution after hydrolysis to the phenol (anion).



**65. Fluorimetric Assay of Hydrolases at Longwave Excitation and Emission Wavelength with New Substrates Possessing Unique Water Solubility, O. S. Wolfbeis and E. Koller, *Anal. Biochem.* **129**, 365-370 (1983). DOI: 10.1016/0003-2697(83)90563-8**

**Abstract.** A direct kinetic fluorometric assay of various hydrolases is described based on new, highly water-sol. substrates. The latter consist of esters of strongly fluorescent 1-hydroxypyren-3,6,8-trisulfonic acid trisodium salt with acetic, butyric, caprylic, and oleic acids. The  $K_m$  and  $V_{max}$  values are given for the hydrolytic activity of various esterases, lipases, acylase I, and chymotrypsin. The figure shows the chemical structure of the type of the virtually nonfluorescent enzyme substrates used. They are converted into strongly green fluorescent products by esterases.

**Figures of merit:** Abs./exc.: 458 nm (log  $\epsilon$  4.3). Em: 512 nm; QY almost 1.0. Decay time: 3 - 5 ns;

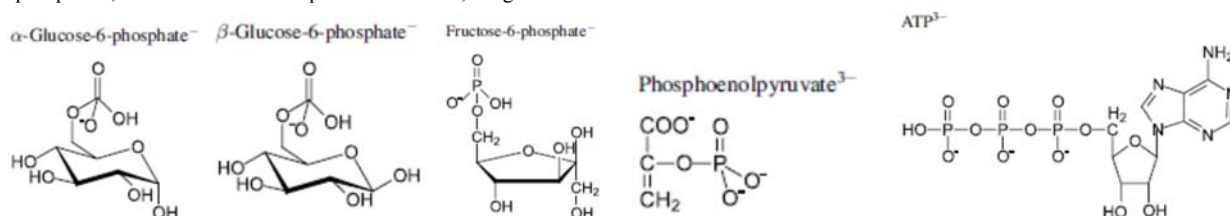




## Section 6. Probes for DNA and (Bio)phosphates (incl. inorganic phosphates)

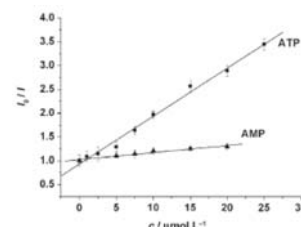
**461. Review: Fluorescent Probes for Microdetermination of Inorganic Phosphates and Biophosphates.** C. Spangler, M. Schaeferling, O. S. Wolfbeis; *Microchimica Acta* (2008), 161, 1-39. DOI: 10.1007/s00604-007-0897-6. IF: 1.6.

**Abstract:** This review covers the progress made in the development of fluorescent probes for inorganic and organic phosphates that are of significance in biosciences. Such probes need to work at physiological pH and at room temperature. The various modes of interactions between probe and phosphate species are discussed, not the least with the aim to assist in the design of more selective probes for which there is a substantial need. Formulae for typical bioorganic phosphates, for which fluorescent probes are known, are given below.



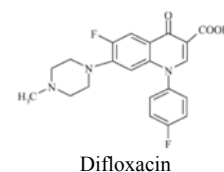
**449. Europium Tetracycline as a Luminescent Probe for Nucleoside Phosphates, and its Application to the Determination of Kinase Activity.** M. Schaeferling, O. S. Wolfbeis; *Chem. – Eur. J.* (2007), 13, 4342-4349. DOI: 10.1002/chem.200601509. IF: 5.0.

**Abstract:** We have studied the effect of a series of adenosine (ATP, ADP, AMP, cAMP) and guanosine (GTP, GDP) phospho-esters, and of pyrophosphate (PP) on the fluorescence emission of the europium tetracycline (EuTC) complex. These compounds have strongly different quenching effects on the luminescence emission of EuTC. The triphosphates ATP and GTP behave as strong quenchers in reducing the fluorescence intensity of EuTC to 25% of its initial value by formation of a ternary 1:1:1 complex. All other phosphates showed a weak quenching effect. The applicability of this fluorescent probe to the determination of the activity of phosphorylation enzymes is demonstrated by means of creatine kinase as a model for non-membranebound kinases. In contrast to other methods, this approach does not require the use of radioactively labeled ATP substrates, additional enzymes, or of rather complex immunoassays.



**445. Sensitive Luminescent Determination of DNA Using the Terbium(III)-Difloxacin Complex.** A. V. Yegorova, Y. V. Scripinets, A. Duerkop, A. A. Karasyov, V. P. Antonovich, O. S. Wolfbeis; *Anal. Chim Acta* (2007), 584, 260-267. DOI: 10.1016/j.aca.2006.11.065. IF: 2.9.

**Abstract:** The interaction of the terbium-difloxacin complex (Tb-DFX) with DNA has been examined by using UV-vis absorption and luminescence spectroscopy. The Tb-DFX complex shows an up to 85-fold enhancement of luminescence intensity upon titration with DNA. The long decay times allow additional detection schemes like time-resolved measurements in microplate readers to enhance sensitivity by off-gating short-lived background luminescence. Optimal conditions are found at equimolar concentrations of Tb<sup>3+</sup> and DFX (0.1 or 1  $\mu\text{M}$ ) at pH 7.4. Under these conditions, the luminescence intensity is linearly dependent on the concentration of ds-DNAs and ss-DNA between 1–1500  $\text{ng mL}^{-1}$  and 4.5–270  $\text{ng mL}^{-1}$ , respectively. The detection limit is 0.5  $\text{ng mL}^{-1}$  for ds-DNAs and 2  $\text{ng mL}^{-1}$  for ss-DNA. The mechanism for the luminescence enhancement was also studied.

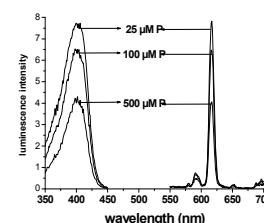


**Figures of merit:** Abs/exc: 340 nm; Em: 545 nm. Best for use in time-resolved assays that can suppress interfering background luminescence.

**428. Microtiter Plate Assay for Phosphate Using a Europium-Tetracycline Complex as a Sensitive Luminescent Probe.** A. Duerkop, M. Turel, A. Lobnik, O. S. Wolfbeis; *Anal. Chim. Acta* (2006), 555, 292-298. DOI: 10.1016/j.aca.2005.09.007. IF: 2.9.

**Abstract:** A new luminescent Eu(III) probe is presented for the determination of phosphate (P) in microtiter plate format. The assay is based on the quenching of the luminescence of the Eu(III)-tetracycline 1:1 complex by phosphate using a reagent concentration of 20.8  $\mu\text{mol/L}$ . The probe is excited at 400 nm and displays a Stokes' shift of 210 nm. The emission maximum is located at 616 nm. The system works best at neutral pH 7. The linear range of the calibration plot is from 5  $\mu\text{mol/L}$  to 0.75  $\text{mmol/L}$  of phosphate, and the limit of detection is 5  $\mu\text{mol/L}$ . The Figure shows the excitation and emission spectra of Eu<sub>3</sub>Tc in presence of various concentrations of phosphate in MOPS buffer of pH 7.

**Figures of merit:** Abs. or exc.: 401 nm ( $\log \varepsilon$  4.2); Em: 616 nm; QY 0.003 in absence of phosphate but 0.05 in its presence. Decay time near 9  $\mu\text{s}$ . This is the Eu(III) 1:1 complex with tetracycline.



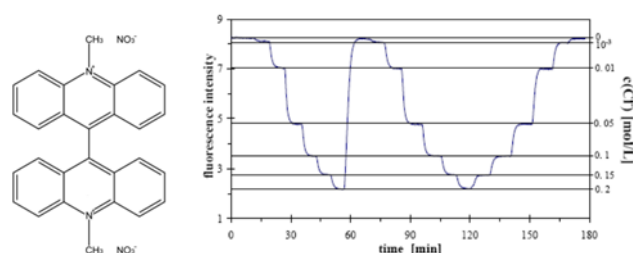


## Section 7. Probes for Halides (mainly chloride)

### 384. Serum Chloride Optical Sensors Based on Dynamic Quenching of the Fluorescence of Photo-immobilized

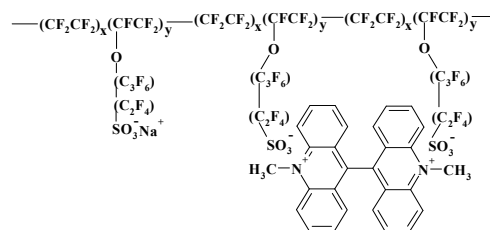
**Lucigenin**, C. Huber, T. Werner, C. Krause, O. S. Wolfbeis; *Microchim. Acta* **142** (2003) 245-253. DOI: 10.1007/s00604-003-0034-0. IF: 1.4.

**Abstract:** We describe an optical sensor for continuous measurement of chloride at extracellular (serum) levels (20 – 200 mM). The sensor is based on dynamic quenching of the fluorescence of lucigenin in a hydrogel. The decrease in fluorescence intensity on exposure to 100 mM chloride typically is -60%. It allows the determination of chloride in the 1 to 200 mM range, with a precision of  $\pm 3$  mM at 120 mM. Bromide, iodide and salicylate interfere, while the effect of pH and oxygen is negligibly small. Response times are in the order of 2 – 5 min. It is used in Roche's blood chloride analyzer.



### 345. Optical Sensor for Seawater Salinity, Ch. Huber, I. Klimant, Ch. Krause, T. Werner, T. Mayr, O. S. Wolfbeis; *Fresenius' J. Anal. Chem.* **368** (2000) 196-202. DOI: 10.1007/s002160000493. IF: 5.7.

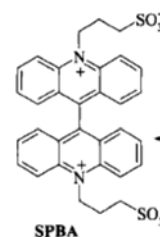
**Abstract:** Seawater salinity (SS) is measured via chloride which is responsible for most of SS. The sensing scheme is based on a fluorescent chloride probe immobilized on a Nafion film. In one approach, the probe undergoes a massive decrease in fluorescence intensity on exposure to chloride ion and this is related to SS. In the second approach, the intensity information is converted into a phase shift information by adding phosphorescent reference particles. The second scheme, referred to as dual luminophore referencing (DLR), is superior. See paper 347. The figure shows a schematic of the electrostatically immobilized chloride probe lucigenin. The graph shows a schematic of electrostatically immobilized lucigenin.



Fluorescent chloride probe immobilized on Nafion

### 332. Anion Induced Fluorescence Quenching of a New Zwitterionic Biacridine Derivative. T. Werner, K. Faehnrich, Ch. Huber, O. S. Wolfbeis; *Photochem. Photobiol.* **70** (1999) 585-589. DOI: 10.1111/j.1751-1097.1999.tb08255.x

**Abstract:** The effect of halides and different buffer anions on the quenching of the fluorescence of the new probe 10,10'-bis(3-sulfopropyl)-9,9'-biacridine (SPBA) has been studied using fluorescence and decay time measurements. The linearity of the Stern-Volmer plot indicates that fluorescence quenching by halides can be described reasonably well by a single-exponential decay with a K of 4.1 times 10<sup>6</sup> M<sup>-1</sup>s<sup>-1</sup> for chloride, 7.83 times 10<sup>6</sup> M<sup>-1</sup>s<sup>-1</sup> for bromide and 1.12 times 10<sup>7</sup> M<sup>-1</sup>s<sup>-1</sup> for iodide. We have found that SPBA is collisionally quenched also by the buffers 3-(N-morpholino)propanesulfonic acid (MOPS) and N-2-hydroxy-ethylpiperazine-N'-ethanesulfonic acid (HEPES). The bimolecular rate constants are 1.67 × 10<sup>6</sup> M<sup>-1</sup>s<sup>-1</sup> for HEPES and 1.44 times 10<sup>6</sup> M<sup>-1</sup>s<sup>-1</sup> for MOPS.



### 68. Fluorescence Quenching Method for Determination of Two or Three Components in Solution, O. S. Wolfbeis and E. Urbano, *Anal. Chem.* **55**, 1904-1906 (1983). DOI: 10.1021/ac00262a016

**Abstract.** The Stern-Volmer equation is extended for cases of 2 or more dynamic quenchers in one solution. The determination of  $n$  quenchers requires  $n$  indicators whose Stern-Volmer consts. have to be different. The concn. of  $n$  quenchers can be computed by solving an  $n \times n$  matrix. The validity of the equations is shown by the precise fluorometric microdetn. of Cl<sup>-</sup> and Br<sup>-</sup> in an org. material after combustion and by the detn. of Cl<sup>-</sup>, Br<sup>-</sup>, and I<sup>-</sup> in a synthetic mixture. The method can be generally applicable for quantifying a variety of dynamic quenchers (ions as well as neutral mols.), if they act independently. Specific indicators are no longer necessary.

$$\begin{pmatrix} \alpha \\ \beta \\ \gamma \end{pmatrix} = \begin{pmatrix} {}^1K_a & {}^2K_a & {}^3K_a \\ {}^1K_b & {}^2K_b & {}^3K_b \\ {}^1K_c & {}^2K_c & {}^3K_c \end{pmatrix} \begin{pmatrix} [Q_1] \\ [Q_2] \\ [Q_3] \end{pmatrix}$$

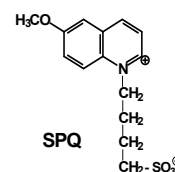
**Figures of merit:** Abs: 347 nm (log  $\epsilon$  3.8); Exc: 450 nm. QY 0.6. Decay time:  $\sim 18$  ns. Widely used quenchable chloride probe; a.k.a. SPQ. Commercially available.

### 66. A Fluorimetric Method for Analysis of Chlorine, Bromine and Iodine in Organic

**Materials.** O. S. Wolfbeis und E. Urbano, *Fresenius Z. Anal. Chem.* **314**, 577-581 (1983). DOI: 10.1007/BF00474851

**Abstract.** A fluorimetric method for determination of Cl, Br, and I is based on quenching of the fluorescence of certain indicators (quinine, 6-methoxyquinoline, acridine, and their derivatives.). The halide ions, formed by combustion of org. halide-containing material according to Schoeniger's procedure, decrease the fluorescence intensity of the indicator. At low halide concentration the quenching obeys the Stern-Volmer law. The method is increasingly sensitive on going from Cl to I. It is suitable for compds. contg. >1% halide. Advantages of the method include (a) a high sensitivity for Br and, esp. I; (b) the lack of a titrimetric procedure; (c) the possibility for automation. The formula shows the chemical structure of sulfopropyl-6-methoxyquinoline which has experienced considerable interest in the past as a chloride-sensitive bioprobe.

**Figures of merit:** Abs: 347 nm (log  $\epsilon$  3.8); Exc: 450 nm. QY 0.6. Decay time:  $\sim 18$  ns. Widely used quenchable chloride probe; a.k.a. SPQ. Commercially available.

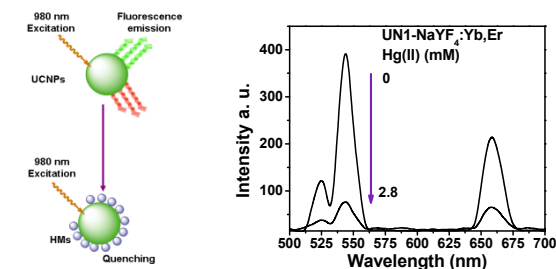




## 8. Probes for Metal Ions (mainly alkali ions and heavy metal ions)

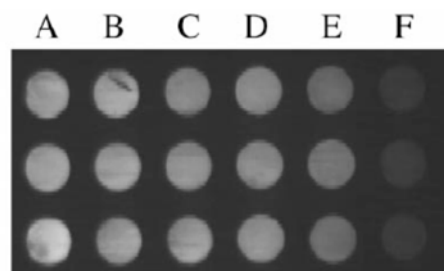
**537. Quenching of the Luminescence of Upconverting Luminescent Nanoparticles by Heavy Metal Ions.** S. M. Saleh, R. Ali, O. S. Wolfbeis; *Chem. – Eur. J.* (2011), 17, 14611-14617. DOI: 10.1002/chem.201101860. IF: 5.5.

**Abstract:** The red and green luminescence of upconverting luminescent nanoparticles (photoexcited with a 980-nm diode laser) is dynamically and statically quenched by heavy metal ions (in particular by Hg(II) ions), and by bromide and iodide. Quantitative quenching studies are presented. The efficiency of quenching is different for the two main emission bands.



**426. Fluorescence Quenching of the Europium Tetracycline Hydrogen Peroxide Complex by Copper(II) and other Metal Ions,** C. Cano-Raya, M. D. Fernández Ramos, L. F. Capitán Vallvey, O. S. Wolfbeis, M. Schaeferling; *Appl. Spectrosc.* (2005), 59, 1209. DOI: 10.1366/000370205774430945. IF: 1.9.

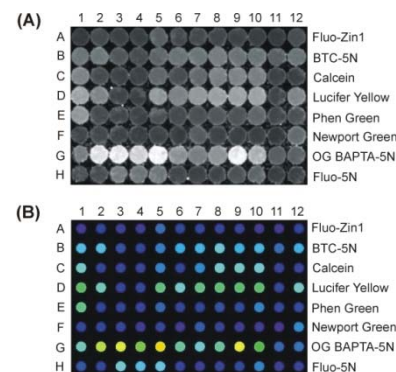
**Abstract:** The europium-tetracycline complex [Eu(Tc)] on addition of hydrogen peroxide (HP) undergoes a 15-fold increase in luminescence intensity. Luminescence is quenched by  $\text{Cu}^{2+}$ ,  $\text{Fe}^{3+}$ ,  $\text{Ag}^+$ ,  $\text{Al}^{3+}$ ,  $\text{Zn}^{2+}$ ,  $\text{Co}^{2+}$ ,  $\text{Ni}^{2+}$ ,  $\text{Mn}^{2+}$ ,  $\text{Ca}^{2+}$  and  $\text{Mg}^{2+}$ . The strongest quenching (both static and dynamic) is induced by  $\text{Cu}^{2+}$ , and these processes were quantified by means of their quenching constants. Stern-Volmer plots were also derived from lifetime imaging measurements accomplished by the Rapid Lifetime Determination (RLD) technique based on microwell plate assays, and also by the Time-Related Single Photon Counting technique (TCSPC). A time-resolved fluorescent method for determination of copper is presented. The response to copper is linear up to 1.6  $\mu\text{M}$ , providing a detection limit of 0.2  $\mu\text{M}$ . The figure shows grey-scale images of solutions of the [Eu(Tc)(HP)] complex in a microwell plate exposed to different concentrations of Cu(II). Data were acquired by the rapid lifetime determination (RLD) method.



**386. Cross-Reactive Metal Ion Sensor Array in a Microtiterplate Format,** T. Mayr, C. Igel, G. Liebsch, I. Klimant, O.S. Wolfbeis; *Anal. Chem.* 75 (2003) 4389-4396.

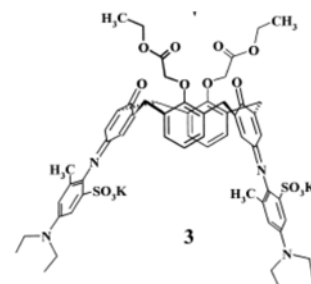
DOI: 10.1021/ac020774t. IF: 5.7.

**Abstract:** A cross-reactive array in a micro titer plate (MTP) format is described that is based on a versatile and highly flexible scheme. It makes use of rather unspecific metal ion probes having almost identical fluorescence spectra, thus enabling (a) interrogation at identical analytical wavelengths, and (b) imaging of the probes contained in the wells of the MTP using a CCD camera and an array of blue-light-emitting diodes as a light source. The response of the indicators in the presence of 5 divalent cations generated a characteristic pattern that was analyzed by chemometry. The fluorescence intensity of the indicators was transferred into a time-dependent parameter applying a scheme called *dual lifetime referencing*. In this method, the fluorescence decay profile of the indicator is referenced against the phosphorescence of an inert reference dye. The intrinsically referenced measurements were performed using blue LEDs as light sources and a CCD camera without intensifiers as the detector (see the graphs below). The pictures obtained form the basis for evaluation by pattern recognition algorithms. Support vector machines are capable of predicting the presence of significant concns. of metal ions with high accuracy.



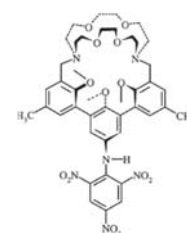
**344. New Longwave Absorbing Chromogenic Calix[4]arene for Calcium Determination in Aqueous Environment.** T. Werner, J. M. Kuerner, Ch. Krause, O. S. Wolfbeis; *Anal. Chim. Acta* 421 (2000) 199-205. DOI: 10.1016/S0003-2670(00)01049-7. IF: 2.9.

**Abstract:** A new calcium ion selective and water-soluble calix[4]arene chromoionophore has been synthesized from the 25,27-bis[(ethoxycarbonyl)methoxy]-26,28-dihydroxy-calix[4]arene (1) and the N4,N4-diethyl-2-methyl-1,4-phenylenediamine-6-sulfonic acid (2). The 1,3-bis(indoaniline)-derived 2,4-bis-[(ethylcarbonyl)methoxy]-calix[4]arene (3) was obtained by introducing sulfonic groups into a phenylenediamine-derived chromophore followed by oxidative incorporation of two units of 2 into 1. The new chromophoric calix[4]arene (formula 3) possesses an absorbance maximum at 604 nm in buffered aqueous environment. Upon complexation of calcium a bathochromic shift of 84 nm occurs along with an increase in the absorption coefficient. The dissociation constants and the cross sensitivity to other alkali and alkaline earth ions were evaluated.



**342. Hydrophilic Sensor Membrane Based on a Cation-Selective Protic Chromo-Ionophore.** Ch. Krause, T. Werner, O. S. Wolfbeis; *Fresenius J. Anal. Chem.* 367 (2000) 426-428. DOI: 10.1007/s002160000390. IF: 5.7.

**Abstract:** The first **potassium** optode based on a protic chromoionophore immobilized in a hydrogel matrix is presented. The highly selective protic chromoionophore consists of a cryptohemispherand moiety and a trinitroanilino chromophore part. The acidifying power of potassium ions over sodium ions is 0.6 pH units. This correlates with the findings in solution. In contrast to several crown and aza-crown based chromophores the highly preorganized moiety allows ion detection even in aqueous environment. The detection limit for potassium ions at pH 7.7 is 5 mM.

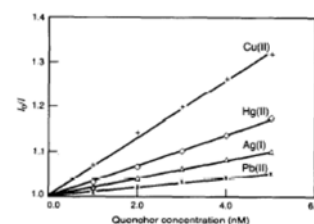
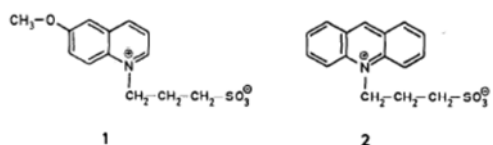




**107. Fluorescence Quenching of Acridinium and 6-Methoxyquinolinium Ion by Pb(II), Hg(II), Cu(II), Ag(I) and Hydrogen Sulfide, O. S. Wolfbeis, W. Trettnak, *Spectrochim. Acta* 43A, 405-408 (1987).**

DOI: 10.1016/0584-8539(87)80125-3

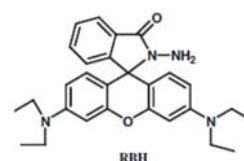
**Abstract.** The quenching of the fluorescence of sulfopropyl-quaternized derivatives of 6-methoxyquinoline (SPQ; 1) and of acridine (SPA; 2) by various heavy metal cations and HS<sup>-</sup> were studied. Stern-Volmer constants were determined, and quenching was found to be exclusively dynamic, except for HS<sup>-</sup>, which acts as both a dynamic and static quencher.



## 9. Probes for Organic Species

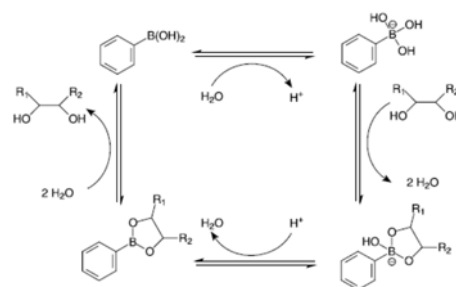
**489. A Fluorescent Probe for Diacetyl Detection. X. Li, A. Duerkop, O. S. Wolfbeis; *J. Fluoresc.* (2009), 19, 601-606. DOI: 10.1007/s10895-008-0450-y. IF:1.8.**

**Abstract.** A water-soluble fluorescent probe, rhodamine B hydrazide (RBH), was prepared and its properties for recognition of diacetyl were studied. The method employs the reaction of diacetyl with RBH, a colorless and nonfluorescent rhodamine B spiro form derivative to give a pink-colored fluorescent substance. In weakly acidic media, RBH reacts more selectively with diacetyl than with other carbonyls, causing a large increase in fluorescence intensity and thereby providing an easy assay for the determination of diacetyl.



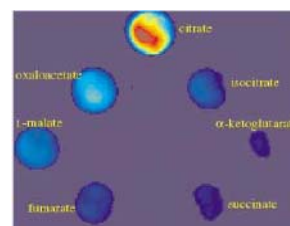
**464. Review: Boronic Acid Based Probes for Microdetermination of Saccharides and Glycosylated Biomolecules. H. S. Mader, O. S. Wolfbeis; *Microchim. Acta* (2008), 162, 1-34. DOI: 10.1007/s00604-008-0947-8. IF: 1.9.**

**Abstract:** This review covers the progress made in the development of fluorescent probes for saccharides and glycosylated biomolecules. Such probes are supposed to work at physiological pH and at room temperature, and preferably have fast responses. The modes of interactions between probe and saccharides are discussed, not the least with the aim to assist in the design of more selective probes for which there is a substantial need. Contains sections on - Unspecific saccharide probes; - Probes for specific determination of glucose; - Probes incorporated into hydrogels and polymers for use in continuous sensing; - Probes for sugar acids and their derivatives; - Probes for determination of glycoproteins; - Boronic acids for probing nucleosides; - Non-fluorescent probes based on boronic acids.



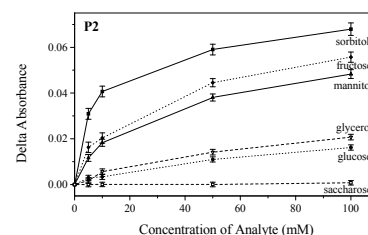
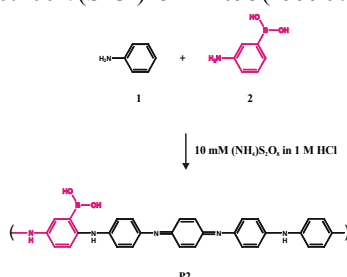
**400. Fluorescent Imaging of Citrate and Other Intermediates in the Citric Acid Cycle, Z. Lin, M. Wu, M. Schaeferling, O. S. Wolfbeis; *Angew. Chem. Intl. Ed.* 2004, 43, 1735-1738. DOI: 10.1002/anie.200353169. IF: 10.3.**

**Abstract:** Citrate and other intermediates of the Krebs cycle (isocitrate, ketoglutarate, succinate, fumarate, malate, oxaloacetate) can be sensed and imaged by time-resolved fluorescence spectroscopy using the Eu<sup>3+</sup>-tetracycline complex as a fluorescent probe. Time-resolutions enables discrimination between different intermediates, and enzymatic conversions are not needed for making the species susceptible to imaging. The complexes with different intermediates can be discriminated via their different "fluorescence" decay times.



**326. A Polyaniline with Near-Infrared Optical Response to Saccharides. E. Pringsheim, E. Terpetschnig, S. A. Piletsky, O. S. Wolfbeis; *Adv. Mater.* 11 (1999) 865-868. DOI: 10.1002/(SICI)1521-4095(199907)11:10<865::AID-ADMA865>3.0.CO;2-B**

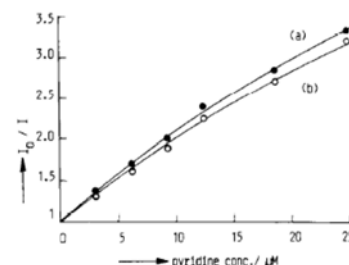
**Abstract:** Copolymerization of aniline and 3-aminophenylboronic acid yields a sugar-binding polymer film whose absorption spectra between 500 and 800 nm undergo large changes on addition of saccharides including saccharose, fructose, glucose, sorbitol, mannitol, and glycerol at neutral pH. The spectral shifts depend on the concentration of the saccharides and are fully reversible, thus allowing continuous sensing. Such films represent an alternative to enzyme-based glucose sensors because of their ease of preparation, compatibility with LED and diode laser light sources, and their thermal and temporal stability. The figure on the left shows the chemistry of the polymerization, and the other the response of the material to saccharides.





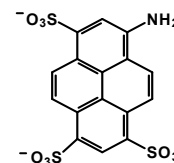
**165. Extremely Efficient Quenching of the Fluorescence of Skatole by Pyridine, A. Sharma, O. S. Wolfbeis, M. K. Machwe, *Anal. Chim. Acta* **230** (1990) 213-215. DOI: 10.1016/S0003-2670(00)82785-3**

**Abstract:** The quenching of the fluorescence of skatole ( $\beta$ -methylindole) by pyridine has been studied in water and ethanol. Extremely efficient quenching is observed, which may be explained on the basis of the formation of a charge-transfer complex between skatole and pyridine. The findings are considered to be of potential utility for the development of methods for the determination of pyridine at sub- $\mu\text{g ml}^{-1}$  levels.



**136. 1-Aminopyrene-3,6,8-trisulfonate: A Fluorescent Probe for Thiamine and Pyridinium Ion, E. Koller, M. Kriechbaum & O.S. Wolfbeis; *Spectroscopy* **3**, 37-39 (1988); *Spectroscopy Intl.* **1**, 44-49 (1988). DOI: 10.1080/00032719208016104**

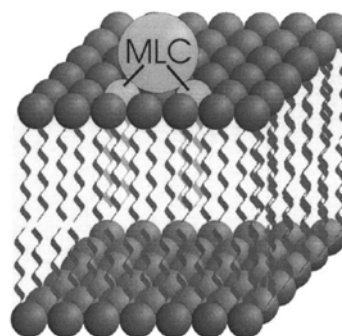
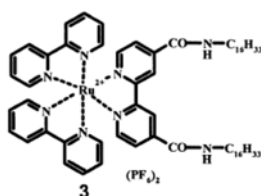
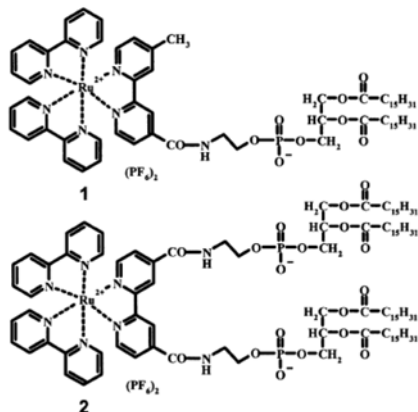
**Abstract:** The quenching of the fluorescence of 1-aminopyrene-3,6,8-trisulfonate (APTS) by the cationic quenchers thiamine, N-cetylpyridinium chloride (CPC), and  $\text{NAD}^+$  was investigated. It was found that CPC and thiamine cause strong static quenching. No changes were observed in the absorption and fluorescence of APTS in the presence of  $\text{NAD}^+$  within the spectroscopically useful concentration range even though  $\text{NAD}^+$  bears a positive charge. APTS is considered to be a useful long-wave absorbing and fluorescence reagent for the fluorometric determination of thiamine and CPC, both of which are virtually nonfluorescent.



## Section 10. Lipid Probes (usually probes for membranes or micelles)

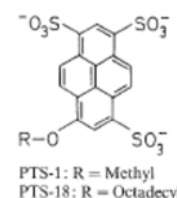
**385. Fluorescence Studies on Fluid Ordered Membranes Using Lipophilic Ruthenium-Ligand Complexes with Long Luminescence Decay Times. C. M. Augustin, O. S. Wolfbeis; *J. Mol. Liquids*, **107** (2003) 141-154. DOI: 10.1016/S0167-7322(03)00146-6.**

**Abstract:** The fluidity of lipid membranes contained in aqueous medium was studied using new fluorescent lipophilic ruthenium-ligand complexes containing dipalmitoyl-glycerophospho-ethanolamine (PE) or hexadecyl side groups, respectively. The new probes display long luminescence decay times and polarized emission, thus making them viable molecular sensors for studying the dynamics and molecular orientation of ordered liquids. Experiments are reported in which the probes were incorporated into lipid bilayers of vesicles, and their luminescence was studied with respect to temperature-dependent emission intensity, decay time and steady-state luminescence polarization. The figures show the chemical structures of the three probes and how the metal-ligand complexes are supposed to become integrated into lipid membranes.



**158. A Sensitive Fluorometric Assay for Cationic Surfactants, S. Marhold, E. Koller, I. Mayer, O. S. Wolfbeis; *Fresenius Z. Anal. Chem.* **336** (1990) 111-113. DOI: 10.1007/BF00322547**

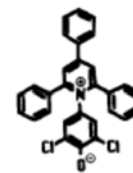
**Abstract:** The fluorimetric assay for cationic surfactants is based on their capability of quenching the fluorescence of 8-octadecyloxy-pyrene-1,3,6-trisulfonate (PTS-18). It is specific for cationic surfactants which can be determined in the 40 - 400 pg concentration range. The method is considered to be advantageous over former methods in that it only requires addition of the sample solution to the fluorophore solution, followed by measurement of fluorescence intensity of the probe. This is in contrast to existing methods where the detergent/dye ion pair has to be extracted before measurement.





**146. ET(33), a Solvatochromic Polarity and Micellar Probe for Neutral Aqueous Solutions,** M. A. Kessler & O.S. Wolfbeis; *Chem. Phys. Lipids* **50**, 51-56 (1989). DOI: 10.1016/0009-3084(89)90025-X

**Abstract.** The prepn. and spectra of ET(33), which is applicable to polarity studies at neutral pH, is described. The probe has a  $pK_a$  value of 4.8 which makes it the first probe of the ET series that exists as a phenolate at near neutral pH. ET(33) shows an extremely large shift in absorption in going from water ( $\lambda_{max}$  409 nm) to THF ( $\lambda_{max}$  646 nm). Spectral properties of ET(33) are studied in various solvents and ethanol-water mixts., and an excellent correlation with standard ET(30) values is obtained. Since the dye is applicable in neutral aq. soln., it is used for detn. of the crit. micellar concn. (CMC) of CTAB at both pH 11 and at near neutral pH. The absorption of the probe is shifted from 409 nm in the sub-CMC range of CTAB to 462 nm at well above the CMC. The very good agreement of the data with literature data demonstrates that ET(33) is a useful and long-wave-absorbing probe for micellar (and probably also lipid) studies at near neutral pH.



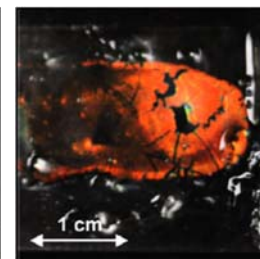
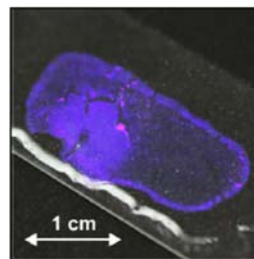
**117. Evaluation of Critical Micelle Concentrations Using New Superpolar Lipid Probes,** M. Kriechbaum, O. S. Wolfbeis and E. Koller, *Chem. Phys. Lipids* **44**, 89-94 (1987). DOI: 10.1016/0009-3084(87)90003-X

**Abstract.** New fluorescent probes (pyranine long alkyl ethers such as 8-octadecyloxy-pyrene-1,3,6-trisulfonate) are presented for the determination of the critical micelle concentration (CMC) of non-ionic detergents. The probes have excellent photostability and are not quenched by mol. oxygen. Both the fluorescence maximum and intensity of the probes change during the transition from monomeric to micellar solns. The environment of this probe in the micelle had a polarity identical with that of MeOH. Cationic detergents cannot be probed because of efficient fluorescence quenching, and with anionic detergents no interaction was observed at all.

## Section 11. Probes for Solvent Polarity

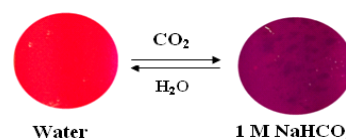
**558. Photonic Crystal Based Sensor for Organic Solvents and for Solvent-Water Mixtures.** Ch. Fenzl, Th. Hirsch, O. S. Wolfbeis; *Sensors (Basel)* **2012**, *12*, 16954-16963 (Special Issue on *State-of-the-Art Sensors Technology in Germany*, 2012). DOI: 10.3390/s121216954. Open access. IF 2.2.

**Abstract:** Monodisperse polystyrene nanoparticles with a diameter of 173 nm were incorporated into a polydimethylsiloxane matrix where they display an iridescent color that can be attributed to the photonic crystal effect. The film is violet in plain water, but turns to red in the presence of the non-polar solvent n-hexane. Several solvents were studied. The films are capable of monitoring the water content of ethanol/water mixtures, where only 1% of water leads to a shift of the peak wavelength of reflected light by 5 nm. The method also can be applied to determine, both visually and instrumentally, the fraction of methanol in ethanol/methanol mixtures. Here, a fraction of 1% of methanol results in a wavelength shift of 2 nm. The reflected wavelength is not influenced by temperature changes nor impeded by photobleaching. The signal changes are fully reversible, and response times are <1 s.



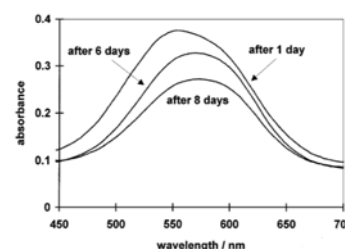
**529. Optical Sensing Scheme for Carbon Dioxide Using a Solvatochromic Probe.** R. Ali, T. Lang, S. M. Saleh, R. J. Meier, O. S. Wolfbeis; *Anal. Chem.* (2011), *82*, 2846-2851. DOI: 10.1021/ac200298j. IF: 5.8.

**Abstract:** The sensing scheme – unlike previous ones that are based on the use of pH indicator probes – is making use of solvatochromic probe Nile Red (NR). Dissolved in a matrix of ethyl cellulose, it can report the polarity of its microenvironment that is modulated by an additive (a hydrophobic amidine) which – in turn – is capable of reversibly binding carbon dioxide. The spectra of NR undergo a strong solvatochromic shift both in color (from brick-red to magenta) and in fluorescence (from orange to red) if the respective sensor layer is exposed to gaseous  $CO_2$  ( $gCO_2$ ) or dissolved  $CO_2$  ( $dCO_2$ ). Both visual and instrumental readout are possible. The detection limits are around 0.23% for  $gCO_2$  and 1.53 hPa for  $dCO_2$ . The response time is in the order of 10 min in the forward direction, and 3 min in the reverse direction for  $gCO_2$ . The optical response also can be quantified using a digital camera by extracting the spectral information contained in the blue and green color channels (in reflectometry), or in the green and red channels (in fluorescence), resp.. Pseudo-color pictures also enable RGB imaging of the spatial distribution of  $pCO_2$ .



**351. Probing the Polarity of Sol-Gels and Ormosils via the Absorption of Nile Red.** A. Lobnik, O. S. Wolfbeis; *J. Sol-Gel Sci. Technol.* **20** (2001) 303-311. DOI: 10.1023/A:1008734320809. IF: 1.0.

**Abstract:** Conventional sol-gels are rather hydrophilic. A more hydrophobic material is obtained preparing organically modified siloxanes (ormosils). The polarity-sensitive probe Nile Red (NR) was doped in various sol-gels to probe their micro-polarity. The experiments show that the NR is an excellent probe and sensitive to the polarity of its microenvironment. Spectroscopic studies reveal remarkable changes in the absorption band positions and intensities as a function of the polarity of the sol-gel, which depends on the different precursors used. Furthermore, sol aging, gelation and temporal stability as a function of different ormosils have been investigated.



**310. Polarity Studies on Ormosils Using Solvatochromic Fluorescent Probes,** A. Lobnik, O. S. Wolfbeis; *Analyst* **123** (1998) 2247-2250. DOI: 10.1039/A804583F



**Abstract:** Ormosils (organically modified siloxanes) are a relatively new family of materials, prepared by the sol-gel method, with properties that are intermediate between those of glasses and polymers. To probe the micropolarity of various solvents and ormosils, a ketocyanine dye (KC) with unique solvatochromic properties in fluorescence was used. KC is an excellent probe and is sensitive to the polarity of its microenvironment. Fluorescence studies revealed remarkable changes in the fluorescence band positions or intensities as a function of the polarity of the ormosil, which depend on the different ormosil precursors used. Storage stability was also investigated.

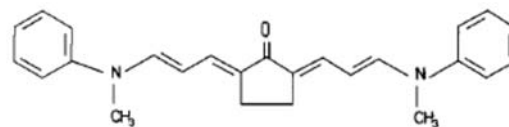
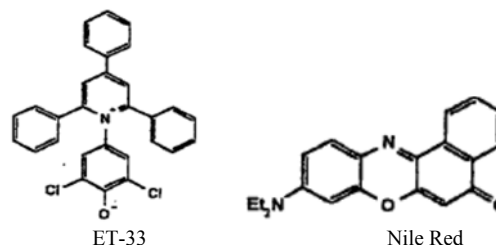


Fig. 1 Structure of ketocyanine dye (KC).

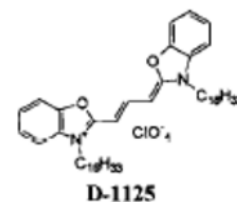
**284. Characterization of Sol-Gel and Ormosils via Polarity-Sensitive Probes, A. Lobnik, O. S. Wolfbeis; *Proc. SPIE*, vol. 3136 (Sol-Gel Optics, IV) (1997) 284-293. DOI: 10.1117/12.284126**

**Abstract:** Conventional sol-gels are rather hydrophilic. A more hydrophobic material is obtained by preparing organically modified siloxanes (ormosils). We have used three different solvatochromic dyes, (1) ET-33, the best solvatochromic probe known so far, (2) Nile red (NR), and (3) a ketocyanine (KC) dye, all with unique solvatochromic properties in both absorption and fluorescence, to probe the micro-polarity of sol-gels. Because ET-33 has a very low molar absorbance and is not fluorescent at all, and KC was hardly soluble in the sol-gel solution, NR was preferably used. NR is an excellent probe and sensitive to the polarity of its microenvironment. Spectroscopic studies reveal remarkable changes in the absorption band positions as a function of the polarity of the sol-gel which depends on the different precursors used. Furthermore, aging time and temporal stability as a function of different ormosils have been investigated.



**262. Fluorescent Potential-Sensitive Dyes for Use in Solid-State Sensors for Potassium Ion, I. Murkovic, A. Lobnik, G. J. Mohr, O. S. Wolfbeis; *Anal. Chim. Acta* 334 (1996) 125-132. DOI: 10.1016/S0003-2670(96)00294-2**

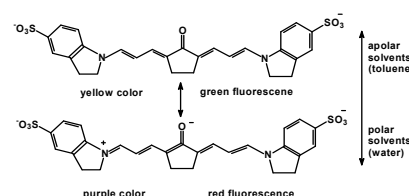
**Abstract:** Fluorescent potential-sensitive dyes (PSDs) were screened for use in potassium-sensitive optical sensor membranes. A potassium-sensitive plasticized PVC layer containing valinomycin as an ion carrier, lipophilic borate salt as an anionic additive, and a PSD was chosen as a model for evaluating the applicability of PSDs. A commercial carbocyanine dye (3,3'-dihexadecyloxycarbocyanine perchlorate) was found to exhibit the best properties in terms of signal changes, photostability and operational life-time. The sensor membrane responds reversibly to potassium ion, with fluorescence intensity changes exceeding 50% and response times being of the order of 1 min. The response to potassium is slightly pH dependent. Typically, an 8% change in intensity is observed over the range pH 5-8. The new sensor membrane exhibits significantly improved signal changes compared to previous optodes based on related sensing schemes. We also report on the effects of different plasticizers and lipophilic additives on the response of the layers. The response mechanism is discussed with respect to the morphology of the membrane.



Formula of a typical dye

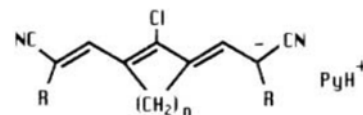
**171. New Highly Fluorescent Ketocyanine Polarity Probes, M. A. Kessler, O. S. Wolfbeis; *Spectrochim. Acta, Part A* 47A (1991) 187-192. DOI: 10.1016/0584-8539(91)80090-6**

**Abstract:** The syntheses and spectral properties of three new and highly fluorescent solvent polarity probes are described. They are found to be extremely sensitive to solvent polarity in that spectral red shifts in both absorption and fluorescence spectra occur upon increasing solvent polarity. The emission data are compared with the standard ET<sup>N</sup> values of solvent polarity and a linear correlation is obtained over a wide range.



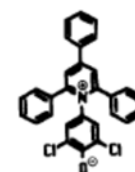
**151. A New He/Ne-Laser Excitable Fluorescent Surfactant Probe, M. A. Kessler, O. S. Wolfbeis; *Ber. Bunsenges. Phys. Chem.* 93 (1989) 927-931. DOI: 10.1002/bbpc.19890930821**

**Abstract.** The fluorescent probe shown at the right is used to probe surfactants and micelles. It can be photoexcited with the He-Ne laser and undergoes a strong increase in fluorescence emission and a longwave shift in the presence of non-ionic and cationic detergents.



**146. ET(33), a Solvatochromic Polarity and Micellar Probe for Neutral Aqueous Solutions, M. A. Kessler & O.S. Wolfbeis; *Chem. Phys. Lipids* 50, 51-56 (1989). DOI: 10.1016/0009-3084(89)90025-X**

**Abstract.** The prepn. and spectra of ET(33), which is applicable to polarity studies at neutral pH, is described. The probe has a pK<sub>a</sub> value of 4.8 which makes it the first probe of the ET series that exists as a phenolate at near neutral pH. ET(33) shows an extremely large shift in absorption in going from water (λ<sub>max</sub> 409 nm) to THF (λ<sub>max</sub> 646 nm). Spectral properties of ET(33) are studied in various solvents and ethanol-water mixts., and an excellent correlation with standard ET(30) values is obtained. Since the dye is applicable in neutral aq. soln., it is used for detn. of the crit. micellar concn. (CMC) of CTAB at both pH 11 and at near neutral pH. The absorption of the probe is shifted from 409 nm in the sub-CMC range of CTAB to 462 nm at well above the CMC. The very good agreement of the data with literature data demonstrates that ET(33) is a useful and long-wave-absorbing probe for micellar (and probably also lipid) studies at near neutral pH.





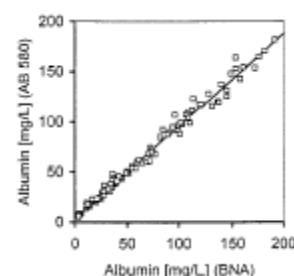
## Section 12. Albumin Probes

### 275. Microalbuminuria and Borderline-Increase Albumin Excretion Determined with a Centrifugal Analyzer and by the Albumin 580 Fluorescence Assay, M. K. Kessler, A. Meinitzer, W. Petek, O.S. Wolfbeis; *Clin. Chem.* **43**, 996-1002 (1997).

DOI: 10.1093/clinchem/43.6.996

**Abstract:** We report on a new automated fluorescence assay for determination of albumin in urine. The dye AlbuminBlue 580 specifically binds to albumin to exhibit strong red fluorescence. The albumin concentration is calculated from emission intensity at 616 nm (excitation at 590 nm) and a calibration curve. Two Cobas Fara programs cover working ranges of 2–200 and 1–50 mg/L with detection limits of 1.4 and 0.4 mg/L, respectively. A test of 100 urine samples submitted to routine analysis gave results that agreed well with those by a nephelometric assay. No interference was detected from other urine components, including several proteins and 46 drugs. The high specificity and sensitivity make the method ideal for determination of microalbuminuria. In addition, the method is fast, inexpensive, and well-suited for clinical laboratory application and thus may be used instead of immuno assays. The figure shows the correlation between the AB 580 fluorescence assay (y axis) and the Behring immuno-nephelometric assay (BNA; x axis) for urinary albumin.

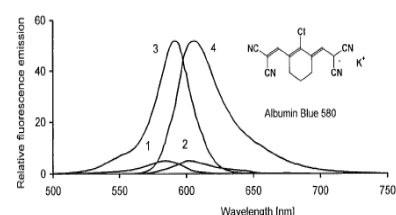
**Figures of merit:** Abs. and exc.: 593 nm (log  $\epsilon$  5.12); but 600 nm in presence of HSA. Em: 608 nm in water, but 630 nm with HSA. More stable than the albumin probes AB633 and AB-670; see below). AB-580 is commercially available from ActivMotif and Sigma-Aldrich. See <https://www.activemotif.com/documents/116.pdf>.



### 270. Albumin Blue 580 Fluorescence Assay for Albumin, M. A. Kessler, A. Meinitzer & O.S. Wolfbeis; *Anal. Biochem.* **248**, 180-182 (1997). DOI: 10.1006/abio.1997.2113

**Abstract:** A new fluorogenic probe for albumin named AB 580 has become available. Its application to the determination of albumin in human serum and urine using an automated analyzer is reported. We also give an assay protocol for a more general application using a conventional spectrofluorometer. The figure shows the formula of AB-580 (with a 6-membered ring!) fluorescence excitation (curves 1, 3) and emission spectra (curves 2 and 4) of AB 580 in pH 7.4 buffer before (1, 2) and after addition (3, 4) of human serum albumin (final conc. 11 mg/L).

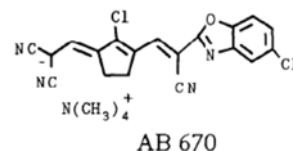
**Figures of merit:** Abs. and exc.: 593 nm (log  $\epsilon$  5.12); but 600 nm in presence of HSA. Em: 608 nm in water, but 630 nm with HSA. More stable than the albumin probes AB633 and AB-670; see below). AB-580 is commercially available from ActivMotif and Sigma-Aldrich. See <https://www.activemotif.com/documents/116.pdf>.



### 188. Laser-induced Fluorometric Determination of Albumin Using Longwave Absorbing Molecular Probes, M. A. Kessler, O.S. Wolfbeis; *Anal. Biochem.* **200**, 254-259 (1992). DOI: 10.1016/0003-2697(92)90462-G

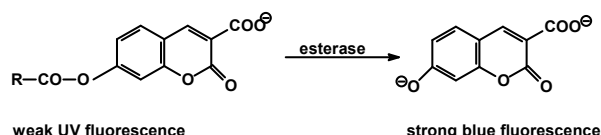
**Abstract:** A novel fluorescence assay for HSA is described. It is based on longwave-absorbing probes that selectively bind to HSA to form fluorescent complexes. The two probes reported here, viz. Albumin Blue 633 (= AB-633) and Albumin Blue 670 (= AB-670) are tailored to match the lines of the 633-nm HeNe laser and the 670-nm diode laser, respectively. In both cases, the strong laser-induced fluorescence of the HSA/probe complexes makes the assay sensitive to HSA at trace levels. Detection limits of 0.2 mg/L were obtained. The assay is highly selective for HSA in that the response to other serum proteins is weaker by a factor of at least 100. Potential interferents are bovine serum albumin (BSA) and some detergents. Parameters of the probe-HSA interaction were obtained from a Scatchard evaluation. The assay presents a promising alternative to immunological determinations of HSA. The chemical formula for AB-633 is similar to the one shown for AB-670 (with a 5-membered ring!), except that the chlorobenzoxazolyl group is replaced by a cyano group.

**Figures of merit:** Abs. and exc.: 648 nm (log  $\epsilon$  5.21) in water, 669 nm in presence of HSA. Em: 668 nm in water; 687 nm in presence of HSA. Low QY in water but higher QY in presence of HSA. Also see *Clin. Chem.* **38** (1992) 2089. DOI: 10.1093/clinchem/43.6.996.



### 124. A Sensitive Kinetic Assay of Serum Albumins Based on Their Enzyme-like Hydrolytic Activity Using a New Chromogenic and Fluorogenic Substrate, A. Gürakar & O.S. Wolfbeis; *Clin. Chim. Acta* **172**, 35-46 (1988). DOI: 10.1016/0009-8981(88)90118-0

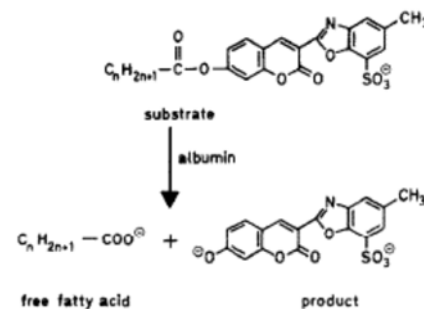
**Abstract.** A new albumin assay, based on the unusual enzyme-like activity of the protein that promotes hydrolysis of ester bonds in fatty acid arylesters was designed for clin. routine use. The substrate introduced shows improved anal. wavelengths and is suitable for both photometric and fluorometric assays. Experiments have been preformed with a conventional photometer, a fluorometer, and an automated analyzer. Detection limits are as low as 10  $\mu$ g/mL photometrically and 20 ng/mL fluorometrically. The method provides a sensitive quantitative determination of even minute amounts. of albumin in liquid solution, and a simple semiquantitative test may be performed by fixing the dye on a test strip which then is immersed into a sample solution and observing the development of yellow color intensity.





**109. The Effect of Fatty Acid Chain Length on the Rate of Arylesterase Hydrolysis by Various Albumins, O. S. Wolfbeis and A. Gürakar, *Clin. Chim. Acta* 164, 329-337 (1987). DOI: 10.1016/0009-8981(87)90308-1**

*Abstract.* A series of synthetic chromogenic and fluorogenic substrates for monitoring the aryl esterase-like activity of albumins from various sources was studied. Except for ovalbumin, all displayed enzyme-like activity. The acetate, butyrate, caprylate, laurate, and palmitate esters of a coumarin dye were found to be efficiently hydrolyzed within the pH range 8.8 - 9.8, with the non-enzymic rate being highest for acetate and lowest for laurate. The latter was considered to be the substrate of choice because it was cleaved most quickly by the proteins tested. A considerable increase in hydrolytic activity was obsd. on addn. of detergents, but not of  $\text{Ca}^{2+}$  and  $\text{Mg}^{2+}$ , whereas addn. of lauric acid to bovine serum album resulted in a 30% decrease in its activity. The results were interpreted in terms of the well-known affinity of albumins for long-chain fatty acids and provide the basis for a sensitive detn. of small amts. of albumins.



.. end